AD_____

Award Number: W81XWH-10-2-0140

TITLE: Development of a Novel Translational Model of Vibration Injury to the Spine to Study Acute Injury

PRINCIPAL INVESTIGATOR: Beth A. Winkelstein, PhD

CONTRACTING ORGANIZATION: University of Pennsylvania,
Philadelphia, PA, 19104-6205

REPORT DATE: October 2013

TYPE OF REPORT: Annual

PREPARED FOR: U.S. Army Medical Research and Materiel Command
Fort Detrick, Maryland 21702-5012

# REPORT DOCUMENTATION PAGE

*Form Approved*
*OMB No. 0704-0188*



| **1. REPORT DATE** *(DD-MM-YYYY)* | **2. REPORT TYPE** | **3. DATES COVERED** *(From - To)* |
|---|---|---|
| October-2013 | Annual | 30September2012-29September2013 |

**4. TITLE AND SUBTITLE**
Development of a Novel Translational Model of Vibration Injury To the Spine to Study Acute Injury

**5a. CONTRACT NUMBER**

**5b. GRANT NUMBER**
W81XWH-10-2-0140

**5c. PROGRAM ELEMENT NUMBER**

**6. AUTHOR(S)**

Beth A. Winkelstein

winkelst@seas.upenn.edu

**5d. PROJECT NUMBER**

**5e. TASK NUMBER**

**5f. WORK UNIT NUMBER**

**7. PERFORMING ORGANIZATION NAME(S) AND ADDRESS(ES)**

University of
Pennsylvania
3451 Walnut Street, P221
Philadelphia, PA 19104-6205

**8. PERFORMING ORGANIZATION REPORT NUMBER**

**9. SPONSORING / MONITORING AGENCY NAME(S) AND ADDRESS(ES)**
U.S. Army Medical Research
And Material Command
Fort Detrick, MD 21702-5012

**10. SPONSOR/MONITOR'S ACRONYM(S)**

**11. SPONSOR/MONITOR'S REPORT NUMBER(S)**

**12. DISTRIBUTION / AVAILABILITY STATEMENT**

Approved for public release, distribution unlimited

**13. SUPPLEMENTARY NOTES**

**14. ABSTRACT**

There is currently little mechanistic data defining the relationship between whole body or spine vibration, physiology and pain. Considering that pain is tremendous problem, we have developed an in vivo model to study how vibration produces chronic pain and the associated effects on tissues and pain cascades. Studies to date have revealed that even 30 minutes of daily vibration for only 7 days is sufficient to induce significant widespread pain that is sustained following the termination of vibration. Moreover, a single day of exposure also induces sensitivity, but the extent of the pain response depends on the frequency of the vibration exposure. Vibration at the resonance frequency of 8 Hz induces pain that lasts for at least 2 weeks, while at 15 Hz it is only transient and recovers by 7 days. This suggests that the exposure periods can drive the pain response and that the duration of the rest-perido that is necessary for symptom recovery depends on specific injury conditions. Similar assays of the tissue responses follow the pain symptoms and recent serum biomarker studies provide a potential readout for injury. Together, all of these findings have tremendous implications for both sub-failure spinal injury and pain. They also establish a strong foundation for the remaining studies including additional exposures and defining the time course of the onset and/or resolution of the physiological responses in a host of tissues including muscle, joints, bones, and brain. Continued investigations in these areas, as well as in the mathematical models we have begun to establish will integrate findings across all tasks of this work.

**15. SUBJECT TERMS**
Pain, vibration, spine, transmissibility, biomechanics, injury

| **16. SECURITY CLASSIFICATION OF:** | | | **17. LIMITATION OF ABSTRACT** | **18. NUMBER OF PAGES** | **19a. NAME OF RESPONSIBLE PERSON** |
|---|---|---|---|---|---|
| **a. REPORT** | **b. ABSTRACT** | **c. THIS PAGE** | | | USAMRMC |
| U | U | U | UU | 44 | **19b. TELEPHONE NUMBER** *(include area code)* |

## Table of Contents

**Page**

## INTRODUCTION

This project combines military injury expertise with pain modeling to develop *in vivo* rat models of painful injury mimicking military injuries, in order to serve as a platform system to understand injury risk, biomechanical mechanisms of painful injury, and to evaluate measures for injury prevention and treatment. In particular, this project is focused on whole body vibration along the spine's axis in repeated loading and after a single exposure of loading. There are three coordinated major activities under this project to ensure we successfully achieve our goals to: (1) identify those schedules of whole body vibration that present the greatest risk for inducing tissue injury, pain and/or changes in spinal mechanics, (2) develop a useful animal model to study these injuries, and (3) establish risk evaluation criteria to identify which injuries and exposures are most threatening. This research project utilizes biomechanical, *in vivo* and biochemical approaches to define injury and pain mechanisms by which repeated vibration and/or single exposures initiate a pain response – either acute or chronic. We proposed an interdisciplinary research approach between collaborators at an academic research institution and the USAARL, in order to develop effective methods to study the most-relevant injuries and to develop a relevant *in vivo* model system would provide such a tool.

In the last year of this project we have made good progress on understanding whole body vibration mechanics in the rat and in establishing several different protocols of whole body vibration that induce sustained and transient pain, separately. We have met the associated timeline of activities and milestones that were laid out in the approved statement of work for this effort. We have also completed critical studies to define the anatomic and mechanical scaling differences between the rat and the human and are implementing them together with ongoing analysis of human data to develop appropriate and meaningful algorithms for evaluating risk for injury as this project moves forward. Lastly, we generated tissues under a variety of exposure conditions to define the temporal development of inflammatory, nociceptive and injury responses. Through such assays of spinal columns, spinal cords, and muscle tissues in the pain-producing scenarios we have uncovered novel relationships between tissue loading, changes in the intervertebral disc, muscle innervation and cascades in the spinal cord, that may contribute to chronic pain in our model. During the past year we also more-deeply investigated and defined the whole body mechanics in our rat model and developed a computational model of rat during vibration to enable more complex research in the absence of using a rat model. In parallel we also investigated the human muscle response and utilized different exposures, such as varied vibration frequencies, along with the ongoing execution of studies to define the temporal tissue responses that will help shape our mechanistic understanding of the pathophysiology of pain from vibration. Moving forward we continue to focus on developing and refining a useful computational model of rat whole body vibration, adding functionality to our current injury device and more completely defining the temporal tissue responses in this model.

## BODY

Over the past year of the project, we have made progress on all of the Tasks that were originally proposed to occur during the third year of our project. Having received approval for the use of human data in our analysis for Task 2 in the prior award period and spending several months last year organizing those data, we made substantial progress on Task 2 this year – particularly focusing on the muscle and transmissibility response of the human during vibration. We have continued to integrate the *in vivo* studies with that work as well and presented findings in 3 presentations at national meetings in the last year, with 2 more to be presented in November 2013. We have published 1 paper, submitted 2 additional papers and are working on 2 additional manuscripts that will be submitted in the next few months.

In this portion of the report we summarize activities related to those publications and refer to the full-publications (provided in the Appendix where amenable), as well as report on the methods and results for the additional studies in detail. A primary goal of this work is to develop *in vivo* rat models of

painful injury from vibration exposures that mimic real-world injuries, in order to serve as a platform system to understand injury risk and biomechanical and biochemical injury mechanisms. Since our last report, the majority of the work has been focused on integrating the anatomic and biomechanical scaling studies with a more developed lumped-parameter mechanical mathematical model to help understand and model our *in vivo* studies, the expansion of the capabilities of our vibration device and data acquisition system, and performing additional *in vivo* studies to determine the effects of different exposure profiles on pain. We also expanded our tissue assays to include assessment of brain responses and to establish protocols to study facet joint, leg bone and serum biomarker responses. In addition, we continue to assay and interpret the finds from our ongoing previous studies. We structure this section of the report to provide an overall summary of each Task and its related status, followed by a more-detailed report of the data and findings for each Task.

The Gantt chart below summarizes the timing of the specific tasks that are associated with each aim across the entire project period under the approved statement of work. Before providing a detailed record of the research findings in the current period, we indicate the current status of each activity in that chart to provide an overview of the research activities that were completed in the previous report, completed during this most recent period, and that are *ongoing* and *planned*.

The majority of activities originally proposed to occur in Year 3 involved performing analysis of human data from the MARS simulations (Aim 1; Task 2) and comparing those biomechanical spine and muscle responses to those in our rat model. That work is currently under review as an invited manuscript submitted to the *Journal of Biomechanical Engineering* [1]. As previously reported, we had initiated selected activities under Aims 3 and 4 in Year 1 and continued to finalize the anatomical scaling studies and developed a computational model of the rat to study biomechanical responses. We also expanded our prior work to establish additional loading conditions for the *in vivo* studies of whole body vibration. We made additional modifications to our device for added utility which also led to work under Task 6. In the last year, we spent greatest effort expanding our sample sizes for tissue assessments, expanding those tissues we assay, and also developing protocols for additional physiological assessments (Aim 3). We also expanded our injury exposure conditions to include a new frequency for the in vivo (Aim 2). Lastly, we have initiated several new assays for tissue responses (Aim 3) and are poised to continue those more in-depth studies in the next year. We have been actively submitting and preparing manuscripts for publication (Task 5) as well. We provide detailed explanation of these and all Tasks in the following detailed summary broken down for each Task.

| **TASK** | **Year 1** | **Year 2** | **Year 3** | **Year 4** |
|---|---|---|---|---|
| **TASK 1 – Obtain Regulatory Approvals (Year 1)** | | | | |
| 1a. Obtain regulatory approval for animal studies | completed | | | |
| 1b. Obtain regulatory approval for use of human data | completed | | | |
| **TASK 2 – Aim 1: Review of Injury Exposures in Theater (Years 1 & 2)** | | | | |
| 2a. Review field data | Completed | | | |
| 2b. Review MARS data | Completed | | | |
| 2c. MARS simulations | | *ongoing & planned* | | |
| 2d. Revise exposures | | *ongoing & planned* | | |
| 2e. Publish findings | Completed | | | |
| **TASK 3 – Aim 2: Design Experimental System & Perform Scaled Loading Studies (Years 1-3)** | | | | |
| 3a. Design initial injury device | completed | | | |
| 3b. Perform scaling studies | completed | | | |
| 3c. Perform pilot studies | completed | | | |

| | | | | | |
|---|---|---|---|---|---|
| with injury device | | | | | |
| 3d. Modify/redesign device | | *ongoing & planned* | | | |
| 3e. Determine loading conditions for in vivo studies | completed | | | | |
| 3f. Perform in vivo studies | | *ongoing & planned* | | | |
| 3g. Perform analysis of mechanics | | *ongoing & planned* | | | |
| **TASK 4 – Aim 3: Injury Studies for Temporal Characterization (Years 2-4)** | | | | | |
| 4a. Identify injury conditions | | | | Completed | |
| 4b. Perform tissue assays for Aim 2 | | | *ongoing & planned* | | |
| 4c. Perform injuries | | | *ongoing & planned* | | |
| 4d. Perform tissue assays for Aim 3 | | | | | *planned* |
| 4e. Integrate findings from Aims 2 and 3 | *ongoing & planned* | | | | |
| **TASK 5 – Publish Findings from Aims 2 & 3 (by end of Year 4)** | | | | | |
| 5a. Identify potential publications | *ongoing & planned* | | | | |
| 5b. Publish findings from Aim 1 | Completed | | | | |
| 5c. Submit findings from Aims 2& 3 | *ongoing & planned* | | | | |
| **TASK 6 – Aim 4: Refine & Simplify Model System for Users (Years 2-4)** | | | | | |
| 6a. Initiate cost-analysis of device design | | *ongoing & planned* | | | |
| 6b. Seek additional funding for prototyping if needed | | | Not needed | | |
| 6c. Initiate analysis of proposed scaling algorithms | | *ongoing & planned* | | | |
| 6d. Integrate injury risk evaluation analysis | | | | *planned* | |
| 6e. Determine risk evaluation algorithms | | | | | *planned* |
| 6f. Complete device development | *ongoing & planned* | | | | |
| 6g. Distribute scaling laws | *ongoing & planned* | | | | |
| 6h. Complete software | *ongoing & planned* | | | | |
| 6i. Produce exposure guidelines | *ongoing & planned* | | | | |

**Task 1**

Work under **Task 1** corresponds to obtaining regulatory approval for both the animal studies (**Task 1a**) and for review of the human data from USAARL (**Task 1b**). In our prior summaries we reported having obtained approval from both the University of Pennsylvania and USAMRMC for the rat studies and an MTA for transfer of the de-identified data (e.g., accelerometer, 3-D position, EMG, force, ECG, internal pressure vehicle acceleration profiles) collected under DAMD17-91-C-1115 'Development of a Standard for the Health Hazard Assessment of Mechanical and Repeated Impact in

Army Vehicles". With both of those regulatory aspects approved previously, **Task 1** also was previously **completed**. There is nothing more to add for this award period.

**Task 2**

Work under **Task 2** corresponds to Aim 1 which includes several sub-tasks of reviewing data related to symptoms (**Task 2a**) and analyzing existing data acquired previously at USAARL (**Task 2b**). Work under **Tasks 2c and 2d** includes running new simulations on the MARS at USAARL, based on the findings from Tasks 2a and 2b. Since approval was previously delayed for review of the human data, work on the remaining Tasks in Aim 1 are also delayed. Accordingly, in the last project period we have focused most activities under Task 2b on deeply analyzing the datasets described in detail in our previous report. In particular, we worked with datasets from USAARL previously collected by the British Columbia Research Inc. (BCRI). Here we detail only those aspects of the methods and results that are new from our previous descriptions (which provided a summary of the test conditions, exposures, etc.). In particular, we focused on characterizing the frequency and muscle responses of seated human volunteers during whole body vibration exposures along the vertical (Z-direction) and anteroposterior (X-direction) directions. Specifically, the transmissibility of the lumbar and thoracic spines was defined for vibration directed along the spine's long-axis (vertically) and in the anteroposterior direction (front-back), in order to define the frequency response of the human. In addition, EMG also was used to measure the corresponding muscle activity in the lumbar and thoracic spines during those imposed vibrations in order to compare the corresponding muscle and resonant responses. Based on prior transmissibility studies and known exposures of workers exposed to whole body vibration [2-9], each exposure consisted of a sine sweep between 2-18 Hz in the Z-direction and X-direction.

All procedures were USAMRMC IRB-approved and performed with informed consent. Prior to participation in the experiments, subjects underwent a focused medical examination. Subjects with a history of back pain or strain, recent trauma or surgical procedures, presence of internal or external prosthesis, and disorders of the muscular-skeletal system were not included in these experiments. Five, healthy, male volunteers (24.8±2.2 years; 73.9±7.3 kg; standing height 1.8±0.1 m) participated in the study. Previously, a portion of the data from these study volunteers was used to develop a repeated jolt health hazard assessment criteria for Soldiers [10,11]. In the current study, unanalyzed biomechanical datasets from these same volunteers during sinusoidal vibration exposures were analyzed.

Each subject underwent separate exposures on different days of whole body vibration directed vertically (Z-direction) and along their front-back (X-direction) while seated (Figure 1). Subjects were seated on a solid metal seat securely mounted on a shaker table (Multi-Axis Ride Simulator; Schenk Pegasus) with a bean-bag cushion taped to the top of the seat pan. The seat was adjusted such that the subject's feet rested comfortably with the hips and knees at approximately 90°. The seat pad was equipped with three, single-axis accelerometers (EGAX-25; Entran Devices) positioned in a tri-axial accelerometer block that measured the input acceleration (Figure 1). Single-axis accelerometers (EGAX-25; Entran Devices) were attached to each subject's skin by a small square (<1 $cm^2$) of two-sided adhesive tape placed over the vertebral processes in the

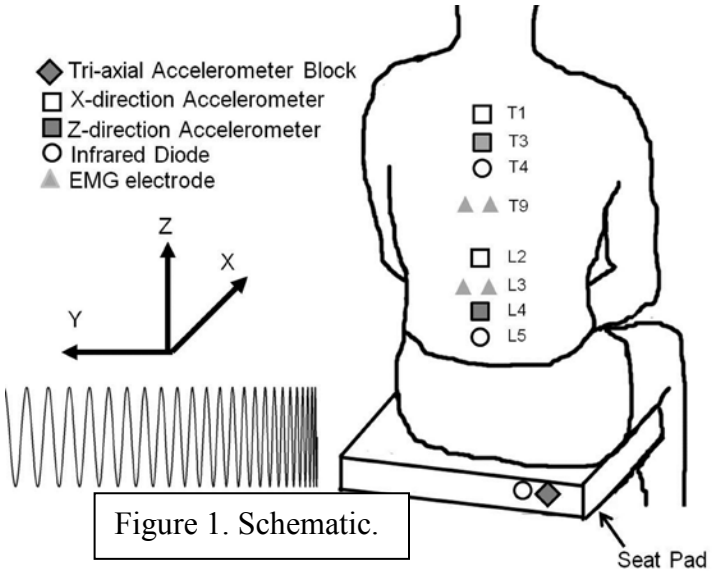


Figure 1. Schematic.

lumbar and thoracic regions (Figure 1). The accelerometers at L4 and T3 were oriented to measure the accelerations along the Z-direction and those at L2 and T1 were oriented at 90° to measure accelerations along the X-direction (Figure 1). In addition, infrared emitting diodes embedded in a plastic coating were attached to the seat pad and the skin over the vertebral processes at L5 and T4 using two-sided adhesive tape, and were tracked using a three-camera system (Optotrak/3200; Northern Digital) positioned 2 m behind the subject. The motions of those lumbar and thoracic markers were measured in all three directions to provide the corresponding three-dimensional displacements of the seat and the spinal regions during each vibration exposure (Figure 1). Acceleration data were acquired at 500 Hz and image data were acquired at 200 Hz.

In addition, for each subject, muscle activity in each spinal region was measured. EMG activity was measured using bilateral surface electrodes (Telemg; Bioengineering Technology Systems) placed symmetrically over the lumbar (L3) and thoracic (T9) paraspinal muscles (Figure 1). An electromyographic amplifier with a high-pass filter set to 10 Hz and a low-pass filter set at 200 Hz was used for all EMG measurements to minimize motion artifact and prevent signal aliasing. On a separate day prior to vibration testing, the maximum voluntary contraction (MVC) for each subject was measured. The pelvis was stabilized during the contractions using 2 canvas cargo straps and a seat belt, and each subject wore a climbing harness attached to a force transducer at chest level (Model U4000, ±100 kg; Maywood Instruments Ltd.). Force and EMG data were recorded while the subject performed a maximal isometric trunk extension in which each subject extended his trunk at the waist against the resistance of the chest harness. The force during extension was recorded as the 100 % MVC force. On the day of testing immediately prior to the vibration exposure, each subject underwent EMG calibration trials by maintaining trunk isometric extension at 40% of the maximum force measured during the prior MVC testing by requiring the subject to sustain brief static contractions at 40% of the maximum force achieved during orientation using real time visual feedback. This was done in order to eliminate the potential muscle fatiguing effect of attempting an MVC prior to testing. The 40% maximum force contraction was used for EMG normalization in analysis. EMG data were acquired at 500 Hz.

Each vibration exposure included a sinusoidal sweep ranging from 2-18 Hz, with a constant amplitude of 0.4 g and lasting for a total of 70 seconds. The hydraulically driven mechanical shaker table was used to impose a sinusoidal sweep in each direction, separately. During each test in the X-direction and Z-direction, acceleration, image, and EMG data were acquired. Only a single direction was tested on a single day, with at least 48 hours of rest between the test days. For both test directions, each of the acceleration, displacement, and EMG signals was segmented into non-overlapping epochs corresponding to distinct seat acceleration input frequencies in order to determine the transmissibility, peak-to-peak displacement, and muscle response.

For X-direction and Z-direction, transmissibility was calculated as the ratio of the root mean square (RMS) of the spinal acceleration to the RMS of the seat pad acceleration in the corresponding applied direction. For each test, the frequency of the seat was calculated using the accelerometer data and spectral analysis in MATLAB. Although seat and spinal displacements were measured through the entire exposure frequency range, only the displacements larger than the system resolution of 0.5 mm (occurring during exposures between 2-5 Hz) were analyzed using Optotrak motion analysis software (Northern Digital). The muscle response for each exposure was determined by calculating the RMS EMG value for each epoch. The muscle responses were normalized by dividing the RMS EMG values measured during testing by the RMS EMG value of the 40% MVC static calibration test and multiplying by 0.4 to scale to the 100% MVC recorded during subject orientation. The normalized RMS EMG approximates muscle activation from zero (no activation) to one (maximal activation), assuming a linear relationship between the EMG signal and the force generated. Assuming bilateral symmetry, the left and right EMG data for each spinal region were averaged together for each vibration exposure.

The acceleration, displacement, and EMG data from all subjects were averaged for each epoch, and transmissibility was determined as a function of the input frequency. The resonant frequency for the

lumbar and thoracic spinal regions was determined using the corresponding acceleration data in that region for each direction. The normalized EMG values for the lumbar and thoracic spinal regions also were compared to the input frequency in each direction of imposed vibration in order to identify those frequencies eliciting the greatest muscle activity. To measure the primary and associated motions of the spine during vibration and to provide context for the muscle data, the peak-to-peak displacements in all three dimensions also were calculated in each spinal region for each subject. For each direction of imposed vibration, separate one-way repeated measures ANOVAs compared the transmissibility and muscle response at each frequency to determine which frequencies produced the greatest responses.

The lumbar and thoracic spinal regions exhibited similar transmissibility responses for these volunteers in the seated position exposed to vibration in both the Z-direction and X-direction, over the range of frequencies (2-18 Hz) tested (Figure 2). The transmissibility of the lumbar spine was higher than the thoracic spine, but both regions exhibited the greatest transmissibility at frequencies below 5 Hz (Figure 2). In particular, for vertically-oriented (Z-direction) vibration, the transmissibility ratio was greater than 1 and significantly higher at 3 Hz ($p<0.002$) and 4 Hz ($p<0.002$) than at any other frequency in both the lumbar and thoracic spinal regions (Figure 2). The peak transmissibility was observed at 4 Hz for the lumbar (transmissibility of 1.61±0.32) and thoracic (transmissibility of 1.49±0.26) regions, but there was no statistical difference between the transmissibility at 3 or 4 Hz for either region (Figure 2). Although a possible second dominant frequency was evident in the lumbar spine between 8-10 Hz, it was not statistically different from all other frequencies. For the X-direction vibrations, the transmissibility ratio in both spinal regions was significantly higher at 2 Hz ($p<0.03$) and 3 Hz ($p<0.03$) than at any other frequency but never exceeded a value of 1 (Figure 2). In both the lumbar and thoracic regions the transmissibility ratio was significantly different at 4 Hz ($p<0.001$), but not higher than 2 Hz and 3 Hz (Figure 2). Even though the transmissibility was a maximum at 2 Hz for both the lumbar (transmissibility of 0.68±0.14) and thoracic (transmissibility of 0.99±0.26) spines, transmissibility was only significantly higher at 2 Hz ($p<0.03$) in the thoracic region and there was no statistical difference between 2 Hz and 3 Hz in the lumbar region (Figure 2).

The muscle responses exhibited similar patterns to the transmissibility responses in both spinal regions (Figures 2 & 3). In fact, the peak muscle response in both spinal regions was detected at the frequency corresponding to the peak transmissibility in each region for both vibration directions (Figures 2 & 3). The peak muscle response in both spinal regions was detected at 4 Hz for the Z-direction vibration and at 2-3 Hz for the X-direction vibrations (Figure 3). In particular, for a Z-direction vibration, the muscle response was significantly higher at 4 Hz ($p<0.05$) than any

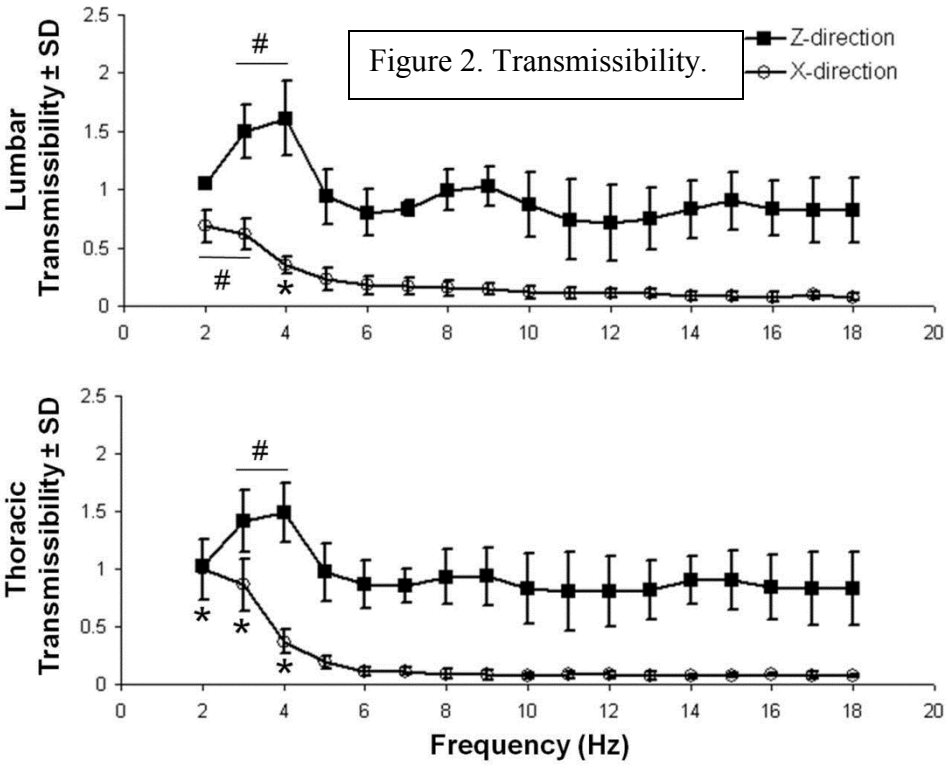


Figure 2. Transmissibility.

other frequency in both the lumbar and thoracic spinal regions; in response to an X-directed vibration, the muscle response at 2 Hz and 3 Hz was significantly higher ($p<0.01$) in both spinal regions (Figure 3). However, the muscle responses at 2 Hz and 3 Hz were not different from each other in either the lumbar or thoracic spines. Interestingly, in the lumbar region the muscle response at 4 Hz was significantly different ($p<0.01$) than all other frequencies for the X-direction test, but was not higher than 2 Hz or 3 Hz.

Figure 3. Muscle responses.

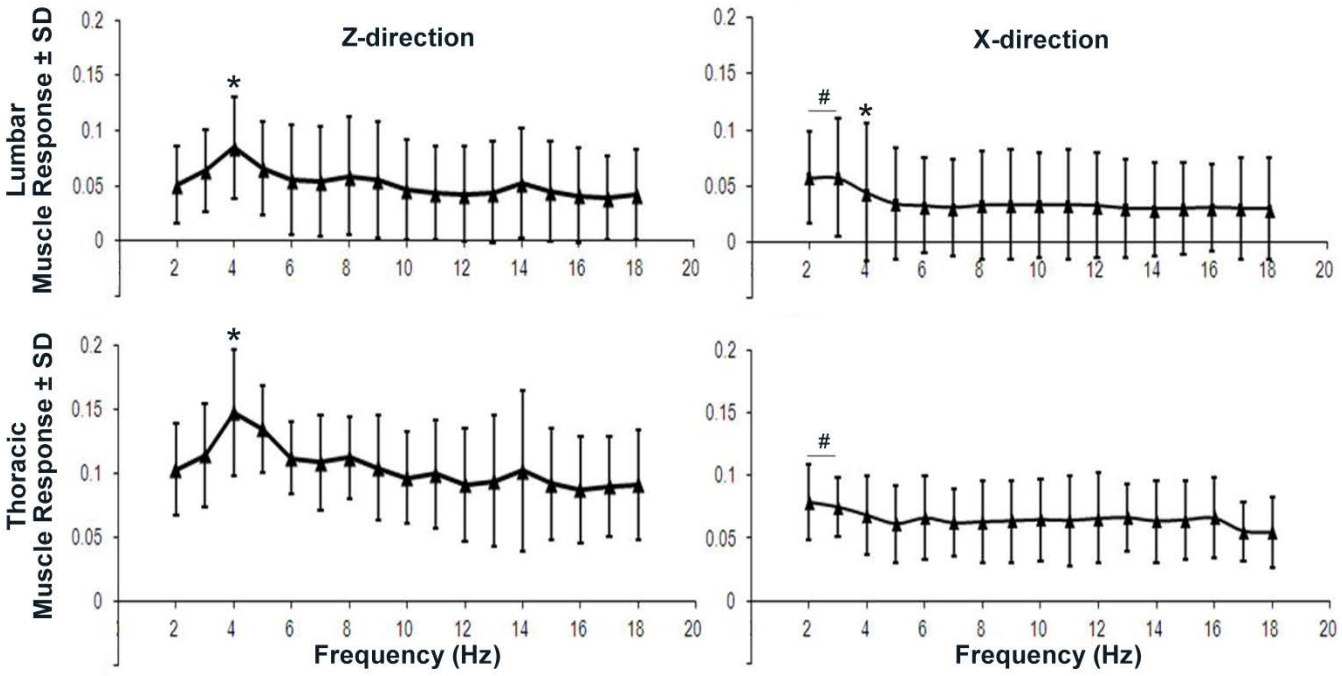


The displacements of the motion markers on the spine for vibrations in the range of 2-5 Hz indicate that the primary motion of each spinal region was in the direction of the imposed seat vibration in all tests (Figure 4). In both vibration directions, there was little motion in the directions that were perpendicular to the primary direction of seat vibration (Figure 4). Although the spinal displacements along the primary axis (Z-axis) during the Z-direction test follow the seat in both spinal regions, there is a slightly greater difference in the lumbar region. Moreover, during a Z-direction vibration, the corresponding Z-direction spinal displacements were greater than the seat displacements at each frequency in both spinal regions (Figure 4). However, the spinal displacements in the X-direction were only greater than the seat displacements in the lumbar region at 2 Hz (Figure 4). For exposures directed along the X-axis, there was greater associated off-axis Z-direction motion in both regions of the spine than were observed for the Z-direction exposures (Figure 4). For both directions of seat vibration, the lateral motions remained negligible (Figure 4).

Figure 4. Displacements.

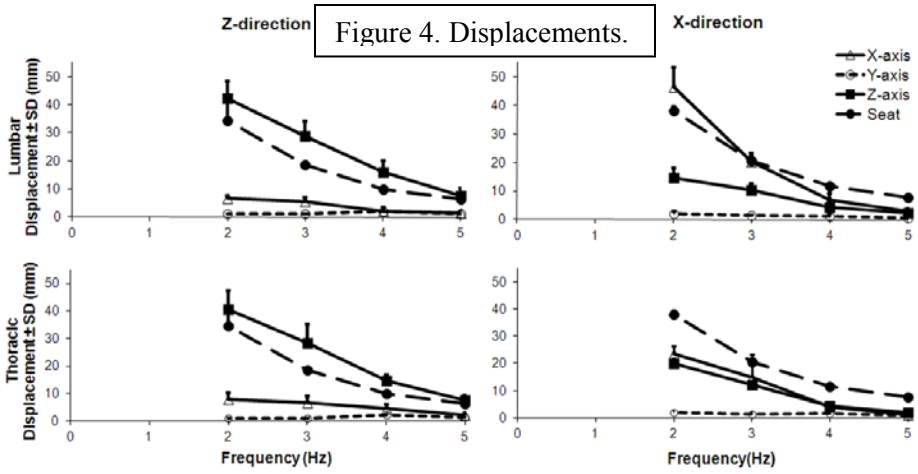

In our previous report we detailed the findings relating the accelerations and transmissibility responses determined using imaging and accelerometer data are in very close agreement at both the thoracic and lumbar levels. Of note, the image-based responses using the Optotrak result in a slightly higher transmissibility value at each frequency but the trends are nearly identical and the degree of variation is the same for both methods of analysis. This is quite encouraging in terms of enabling future interpretation and integration with other studies using only one or the other method of tracking whole body mechanical responses to vibration.

We continue to work with USAARL to analyze other aspects of these datasets. In particular, we continue with activities under **Task 2c** and **Task 2d.** In addition, we jointly co-authored an abstract presented at the *ASME-BED Conference* in June 2013 (see Appendix A1), which was awarded the 3rd place prize for the student paper competition, and have submitted a manuscript that is currently under review at *the Journal of Biomechanical Engineering*.

**Task 3**

Work under **Task 3** corresponds to Aim 2 of the proposal and focuses on refining our experimental methods to impose controlled vibration in vivo and to evaluate pain and functional outcomes for loading to the neck and low back. With **Tasks 3a-3c** completed in prior reports, and the device and exposure conditions established for imposing vibration, efforts in this task in the last year focused primarily on refining several specific exposure protocols and implementing several new aspects to the model to assess additional behavioral responses and to investigate an additional vibration frequency based on our prior mechanical studies (**Tasks 3d, 3f, 3g**). For brevity we do not re-describe our system since it was described in great detail in prior reports and can be found in our recent publication [12] (see Appendix A2 for preprint). Further, based on that prior work, we also elected to investigate effects of using a 8 Hz vibration since we have previously identified it as the resonance frequency of the rat.

Based on our prior behavioral and mechanical studies, we recently modified our existing device to enable more robust stroke distances, accelerations and data acquisition (Figure 5). All other aspects of our protocols are the same. We performed several biomechanical studies to assess accelerations of the plate and the rat, to ensure transmission of known inputs to the rat. A summary of those mechanical studies is provided in Appendix A3).

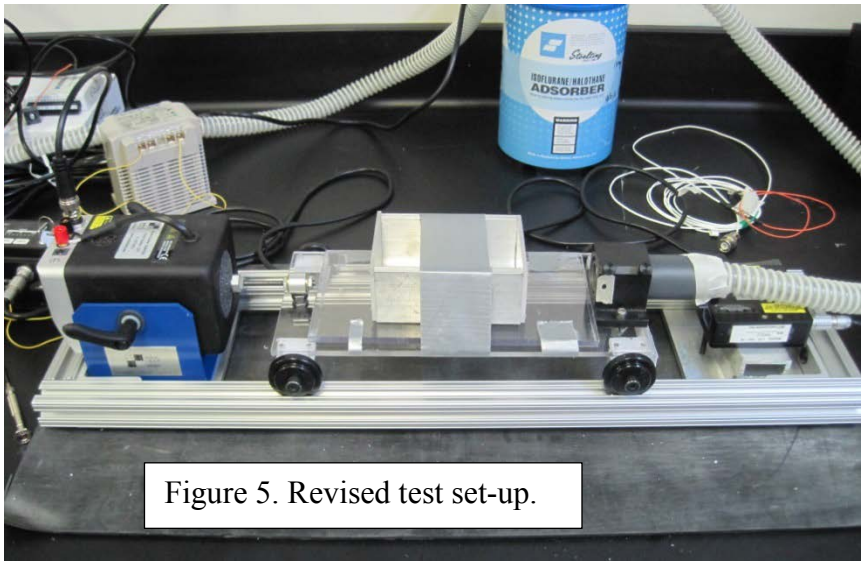

Figure 5. Revised test set-up.

In addition, we have recently used that set-up to perform impose 8 Hz vibration exposures. Separate groups of rats were exposed to either an intermittent vibration applied only on 2 days with a rest-period between them (n=7) or a sham exposure on those two days (n=4). For each vibration exposure, the rat was vibrated at 8 Hz with an acceleration of 3.8±0.12g for 30 minutes. A sham control group (n=4) underwent anesthesia treatment matching the same timing of the intermittent vibration group. All other specific methods are the same as previously described in prior reports.

Behavioral sensitivity was assessed by measuring mechanical hyperalgesia in the forepaws and hindpaws on all days, as previously [12]. Interestingly, sustained hypersensitivity was induced in both the hindpaw and forepaw (Figure 6). Vibration exposure induced significant sensitivity in both paws as early as day 1 after the first exposure that was maintained for all days ($p<0.05$). This was different than what was previously observed for two single exposures at 15 Hz (Figure 6), suggesting that exposure at the resonance frequency may be more injurious than at other frequencies. We continue to perform these studies and increase the time points for tissue harvest, as well as define the specific biomechanical responses for this exposure.

Figure 6. Pain behaviors.

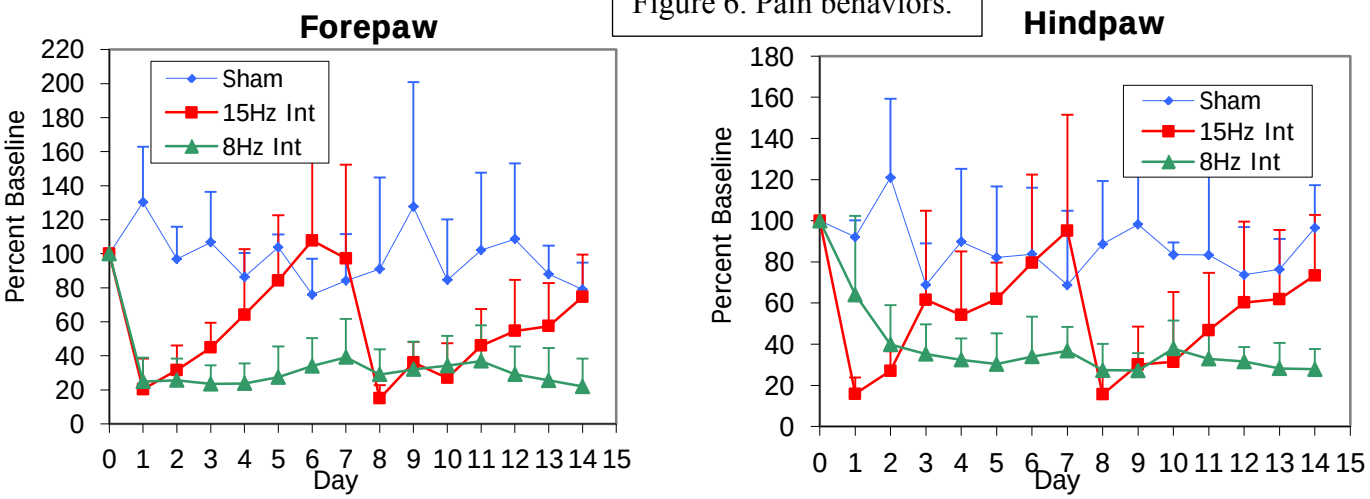


Similarly, as our analyses of the biomechanical responses of the rats during vibration progressed, we became interested in assessing if there are associated injury and/or trauma to the brain as a result of this low-level repeated vibration. In order to begin to assess the extent of headache in our model, we began assessing sensitivity to mechanical stimuli applied to the occipital region of the head. We used customary measurement techniques which we have previously established for measuring TMJ sensitivity [13]. We assess such responses in three groups of rats: sham (n-3), a 15 Hz vibration applied for 7 days (n=4) and 8 Hz vibration applied on days 0 and 7 (n=7). No sensitivity was developed in the sham animals (Figure 7). However, the repeated exposures induced significant increases in sensitivity ($p<0.0001$) during the exposure period, which was only sustained for 2 days after the exposure (days 7 & 8) (Figure 7). In contrast, a single 8 Hz exposure induced such sensitivity on all days of testing (Figure 7). We continue to investigate potential effects on the brain in coupled tissue assays; we summarize those additional findings under **Task 4**.

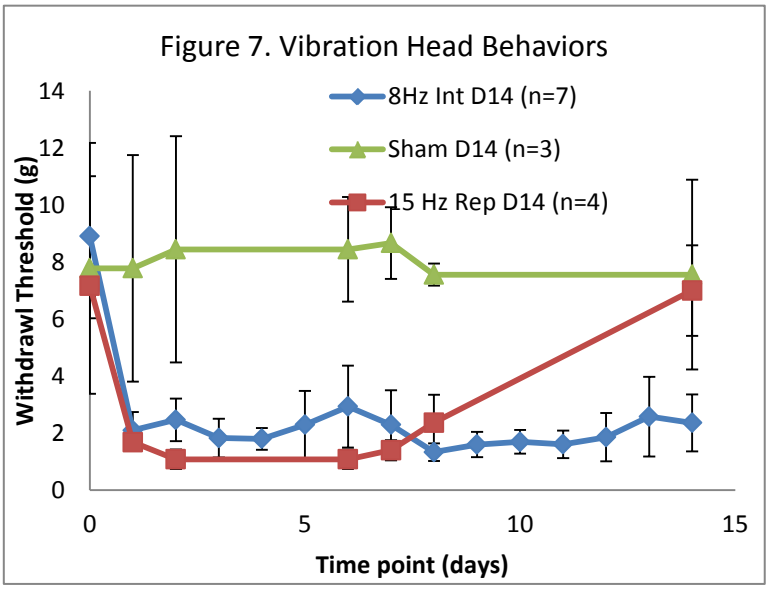


**Task 3b** focuses on establishing scaling criteria between the rat and human. As previously described our work in that Task focused on two areas which have largely been completed: (1) defining the anatomy and geometry of the rat spine in order to compare the size, shape and relationship of anatomical features to the relevant anatomical features of the human and (2) developing a mathematical model of the rat spine for vibration along the long-axis of the spine in order to investigate aspects of this model system for easy comparison to the

human. In the last year, we have been working on writing up the findings that were described in the previous report and are preparing a manuscript that will be submitted in the next few months. The mechanical modeling work is ***ongoing*** since we are integrating these findings with the mechanical studies in **Task 3g**.

**Task 3e** was generally **completed** during last year and reported in our prior submission. However, based on the work we previously reported that determined the resonancy frequency of the rat to be at 8 Hz, we have also recently expanded out prior work with 15 Hz. Here we detail both such in vivo conditions, with reference to the publication detailing the behavioral and mechanical data from the 15 Hz exposures, which was summarized in detail in our previous report. We provide the more detailed summary of our recent work with the 8 Hz exposure as that has yet to be published. We continue work with both conditions, especially in the intermittent exposure and are poised to undertake studies with a single jolt. These studies are ***ongoing and planned*** in order to determine and define the full set of loading conditions under **Tasks 3f and 3g**.

In addition to the analysis of the kinematics and kinetics already described above for the vibration studies in vivo and the transmissibility studies (that were described in detail in a previous report) under **Tasks 3b and 3g**, we have continued the ongoing efforts to develop lumped mass models simulating our vibration system. Over the last year we presented our working mechanical-analog models of the vibrated rat with mass-springs-dampers systems at the *ASME-BED Conference* in June 2013 (see Appendix A4) and optimized the parameters of the model as well as performed validation studies with experimental conditions.

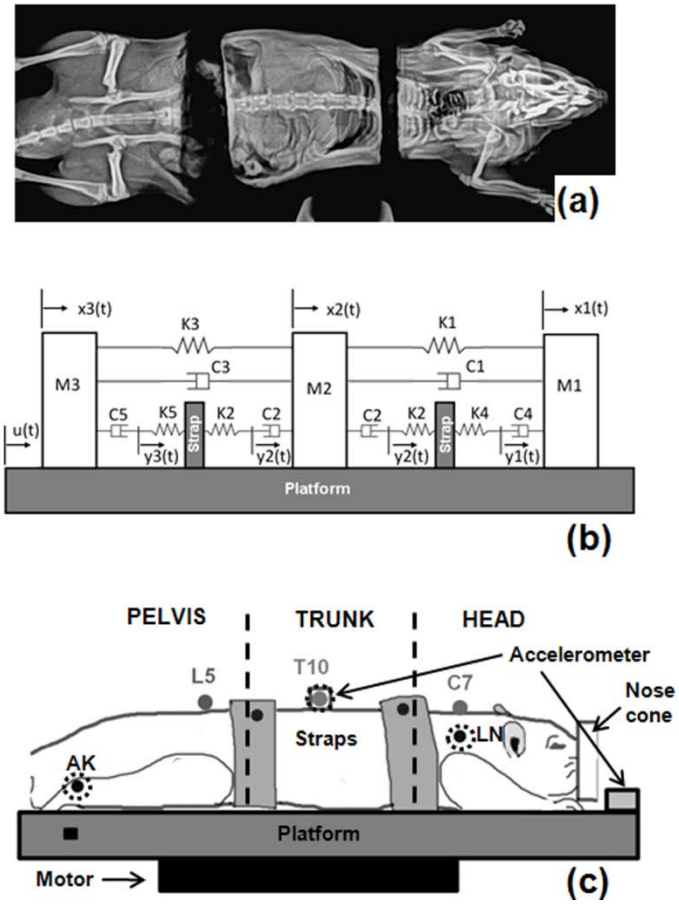


Figure 8. Model.

A 3DOF lumped-parameter model of a rat attached to a vibrating platform by two straps was constructed with three masses representing the head and shoulders (M1), trunk (M2), and the pelvis and legs (M3) (Figure 8). To quantify the distribution of mass between these three body segments, expired frozen rats (n=9; 361±19g) were sectioned at the location where the straps were applied in the vibration (T8-T9 & L4-L5) and each segment was weighed in order to determine average relative masses of each (Fig. 1a). The mass of the head/shoulders, trunk, and pelvis/legs represents 26±2.4%, 37±4.3% and 36±2.9% of the total body mass of the rat, respectively. Springs and dampers were used to model the connections between the masses, simulating the nonlinear mechanical behavior of the hard and soft tissues between each of the body segments ($K_1$, $K_3$; $C_1$, $C_3$) and between each of the body segments and the straps ($K_2$, $K_4$, $K_5$; $C_2$, $C_4$, $C_5$) (Figure 8b). The system of differential equations (eq. 1) describing the model was solved for the theoretical displacements of the masses ($x_1$, $x_2$, $x_3$) as a function of the masses, spring coefficients, damper coefficients, and motion of the platform, u (Figure 8c).

$$-K_1(x_1 - x_2) - C_1(\dot{x}_1 - \dot{x}_2) - C_4(\dot{x}_1 - \dot{y}_1) = M_1 \ddot{x}_1$$
$$K_4(y_1 - u) = C_4(\dot{x}_1 - \dot{y}_1)$$

$$-K_3(x_2 - x_3) - C_3(\dot{x}_2 - \dot{x}_3) - C_2(\dot{x}_2 - \dot{y}_2) + K_1(x_1 - x_2) + C_1(\dot{x}_1 - \dot{x}_2) + C_2(\dot{y}_2 - \dot{x}_2) = M_2 \ddot{x}_2 \quad \text{eq. 1}$$
$$K_2(y_2 - u) = C_2(\dot{x}_2 - \dot{y}_2)$$

$$K_3(x_2 - x_3) + C_3(\dot{x}_2 - \dot{x}_3) + C_5(\dot{y}_3 - \dot{x}_3) = M_3 \ddot{x}_3$$
$$K_5(u - y_3) = C_5(\dot{y}_3 - \dot{x}_3)$$

Vibration was applied to male Holtzman rats affixed to the rigid platform via straps (Figure 8c), as previously described above to provide the displacements of the body segments (M1-M3) during whole body vibration for the development of the lumped-parameter model. Briefly, rats underwent sinusoidal vibrations with a 1.5 mm peak-to-peak amplitude, ranging from 3-15 Hz in 1 Hz increments. A high-speed camera (0.035 mm spatial resolution; 120 Hz) tracked the eye and markers placed on the head/neck, trunk, pelvis/leg, and the platform (Figure 8c). Displacements were measured using a tracking software (ProAnalyst; Xcitex) and were used to compute the transmissibility for each body segment. Uniaxial accelerometers (Model 7521A2; Dytran) affixed to the platform and the thoracic spine of the rat (Figure 8c) recorded accelerations along the spine at 120 Hz during each exposure.

Expired rats (n=4; 379±11g) underwent WBV at each frequency, and the transmissibility of each body segment was calculated as the ratio of the root-mean square (RMS) displacement of that body segment over the RMS displacement of the platform. For these experimentally-derived transmissibility responses, markers on the lateral neck (LN), trunk (T10), and ankle (AK) were tracked for each segment, respectively (Figure 8c). Notably, the LN and AK markers were drawn on the skin, whereas the T10 marker was on the accelerometer that was rigidly pinned to the thoracic spine.

These same transmissibility responses were also calculated from the model using different values of the K and C parameters, repeated iteratively until the goodness-of-fit (ε)) between the theoretical and experimental transmissibilities was at least 0.85. A sensitivity analysis also was conducted with the K ranging between 1-1000 N/m and C ranging between 1-50 (N.s/m) to evaluate the influence of their variation on the goodness-of-fit. The theoretical transmissibility for each body segment was compared to the corresponding experimental transmissibility using an F-test with a 95% significance. The set of K and C parameters yielding the highest value of ε (Appendix A5) was used in the optimized model, which was validated and used to predict spinal motions and trunk accelerations.

In order to both validate the optimized model and to evaluate the effect of marker location on the transmissibility, a separate group of expired rats (n=5; 436±20g) underwent the same vibration protocol and data analysis as above twice, with markers placed on the skin and then directly on the spine. In the skin-based configuration additional markers were pinned to the skin at the C7 and L5 spinal levels while the trunk accelerometer (T10) was strapped to the animal. In the spine-based configuration, the C7 and L5 markers and trunk accelerometer were all directly pinned to the spine at their respective anatomic location (Figure 8c). The experimental transmissibilities measured with the skin-mounted C7 and L5 markers and the spine-mounted accelerometer were respectively compared to the head, pelvis, and trunk transmissibilities predicted by the optimized model for its validation, using an F-test with a 95% significance. The skin-based transmissibilities obtained at C7, T10, and L5 were compared to the spine-based transmissibilities at these same spinal locations using an F-test with a 95% significance, which enabled evaluating the effect of markers' attachment. In addition, the skin-based transmissibilities at C7 and L5 were also compared to the transmissibilities at the lateral neck and ankle, respectively, to estimate the influence of marker location on the transmissibility measurements.

Cervical and lumbar motions were predicted using the optimized model as the differences in the displacements of adjacent masses, $x_2$-$x_1$ and $x_3$-$x_2$, respectively. The trunk RMS acceleration was derived from the predicted trunk displacement. The spinal motions from the experiments were taken as the difference between the ankle and T10 marker displacements for the lumbar region, and between the

T10 marker and eye displacements for the cervical region. The experimental RMS acceleration was directly measured by the trunk accelerometer. The predicted outcomes were each compared to the experimentally-derived values obtained from vibrating anesthetized rats at both 5 Hz and 15 Hz (n=10; 299±11g) using an F-test with a 95% significance.

The goodness-of-fit was greater than 0.85 for all $K_1$ and $K_3$ coefficients ranging from 100-1000 N/m, and $C_1$ and $C_3$ coefficients ranging from 3-50 N.s/m (Figure 9a-f). Yet, variation between 100-300 N/m from the optimized $K_2$, $K_4$, $K_5$ coefficients produced a substantial decrease in the goodness-of-fit. This substantial drop in ε was also observed for variations ranging 8-10 N.s/m from the optimal $C_4$ and $C_5$ coefficients (Figure 9a-f). Based on these findings, the optimal K and C coefficients were selected, with associated goodness-of-fits of 0.92, 0.91, and 0.89 ($F \geq 0.46$; $Fc=0.35$) between experimental and theoretical transmissibility responses for the head, trunk, and pelvis, respectively (Figure 9g-i).

The model did not accurately predict spinal motions, moderately predicted transmissibilities but precisely predicted trunk acceleration. The transmissibilities predicted by the optimized model were significantly different from those defined experimentally ($F \leq 0.30$; $Fc=0.35$), especially at C7 and T10 despite goodness-of-fits of 0.61 for C7, 0.74 for T10, and 0.85 for L5 between the theoretical and experimental transmissibilities (Figure 10). The model tended to overestimate the transmissibilities for frequencies between 5 and 9 Hz and underestimated the resonance frequency (Figure 10). For example, the predicted maximum transmissibility at C7 was 40% greater than that determined experimentally (Figure 10c). The model predicted a resonance frequency of the trunk (T10) at 8 Hz, but it was found to be at 9 Hz using experimental data (Figure 10b).

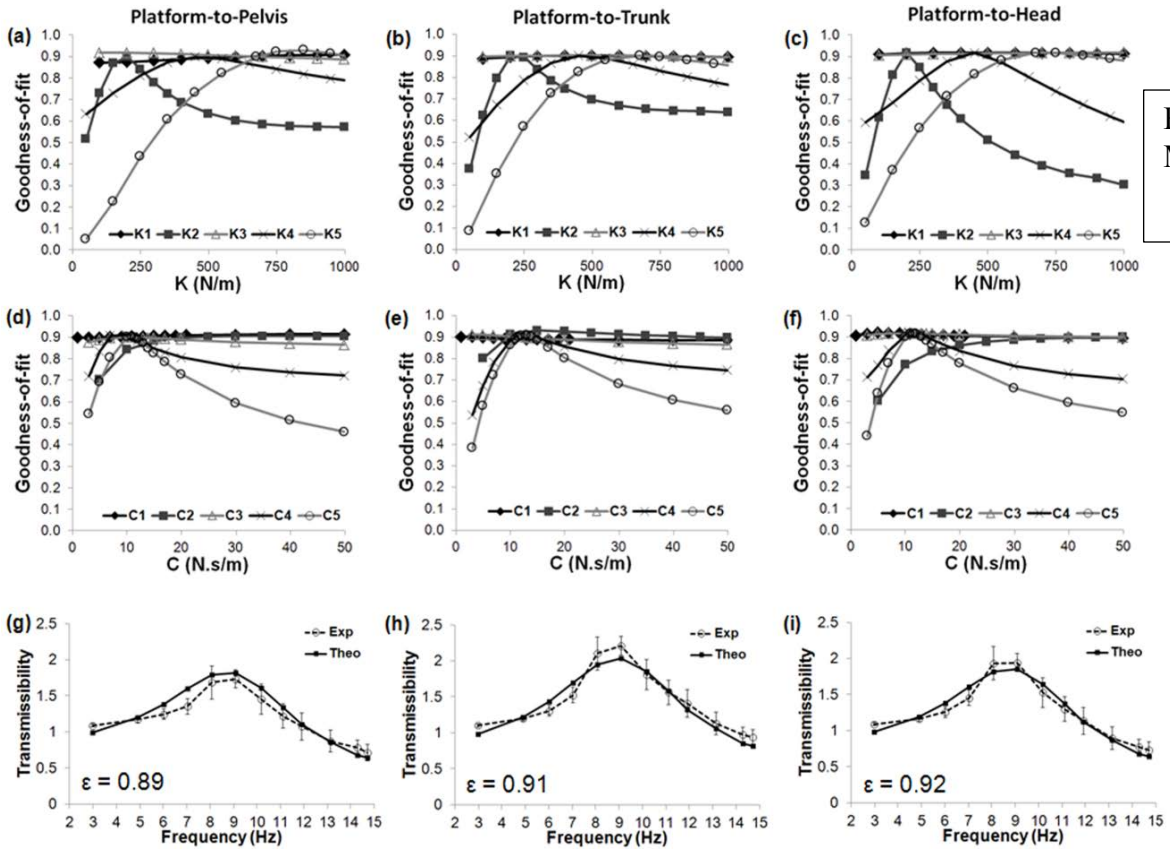


Figure 9. Model fits.

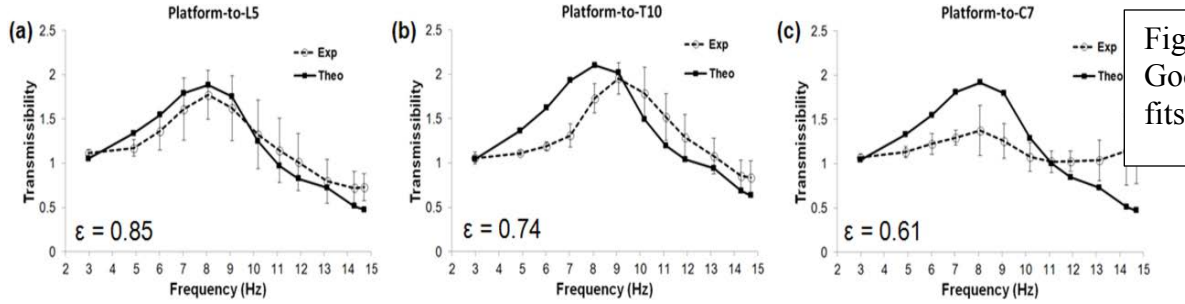


Figure 10. Goodness of fits.

The predicted RMS trunk acceleration at 5 Hz (1.1 $m/s^2$) was significantly less ($p<0.01$) than that measured experimentally, but for the 15 Hz vibration the estimated (6.1 $m/s^2$) and experimental (6.2 $m/s^2$) accelerations were in very good agreement (Figure 11). The model consistently underestimated spinal motions in both compression and extension for both frequencies (Figure 11). For a 5Hz vibration, the magnitude of the predicted cervical extension and lumbar compression was more than 5 times smaller than the experimental motion (Figure 11). Overall, the model did best at predicting lumbar extension at 5Hz (Figure 11). Despite the differences between predicted and experimental spinal motions, cervical extension and lumbar compression for a 5Hz vibration were the only motions that were significantly smaller ($p<0.01$) than their respective experimental values (Figure 11).

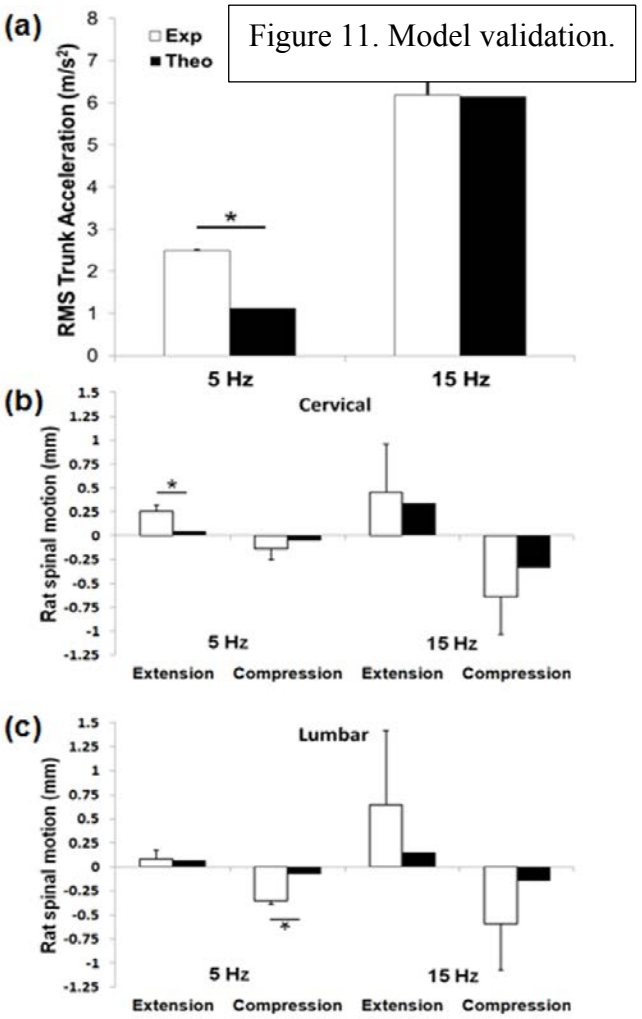


Figure 11. Model validation.

The resonance frequency and transmissibility amplitude from the skin-based measurements were significantly smaller ($F<0.01$; $Fc=0.35$) than for the spine-based measurements for C7 and T10 (Figure 12). However, the transmissibilities for L5 were not significantly different ($F=0.86$) (Figure 12). Similarly, there was a significant difference between the transmissibilities determined from the skin-mounted lateral neck (LN) and the skin-mounted C7 markers ($F<0.01$; $Fc=0.35$) (Figure 13). But, there was no difference between the transmissibilities measured using the skin-mounted ankle (AK) and L5 markers ($F=0.71$) (Figure 13).

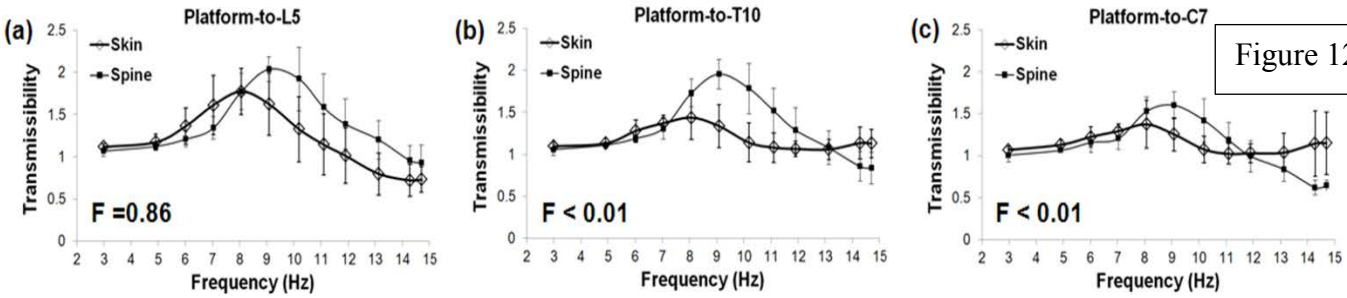


Figure 12. Fits.

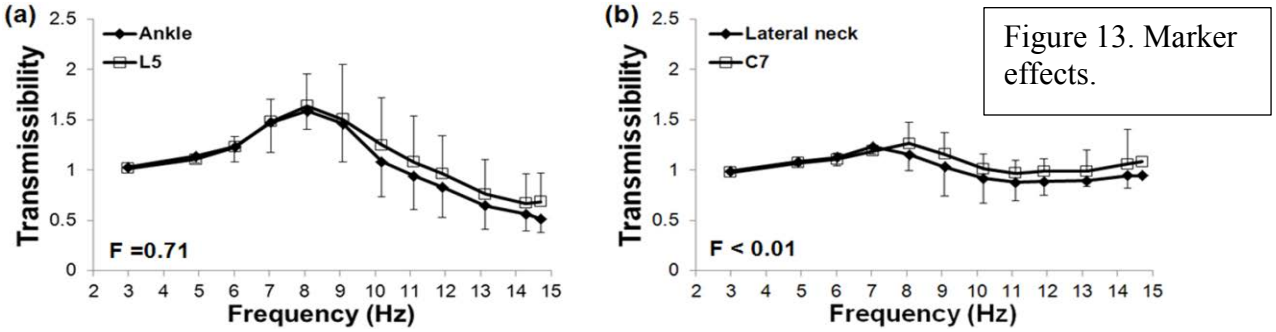


Figure 13. Marker effects.

Based on these results and the apparent utility of our model, we continue to refine the model in coordination with our anatomic studies to move towards including more tissue-level resolution. A manuscript describing this model has been submitted and is under review. Activities under **Task 3g** are ***ongoing*** and will be continue in the next year.

**Task 4**

Work under **Task 4** corresponds to Aim 3 which involves the temporal characterization of responses in relevant tissues in the periphery (appendages), spine, and central nervous system (spinal cord and brain) after vibration exposure. In the past year we continued to generate those tissues for relevant time points for the whole body vibration exposures (daily and intermittent exposure models, both 15 Hz and 8 Hz) and also expanded our assays to include brain, leg bone, facet joints and blood serum. Of note, **Task 4a** is ongoing and planned with regards to the specific jolt injury condition, but with the injury conditions of the whole body vibration already defined under **Task 3**, we are active in generating tissue for those injury conditions under **Tasks 4b-4d**. Work with the jolt exposures are planned for initiation in the next year.

At each time point of tissue harvest, we collect a variety of tissues, including the brain, cervical and lumbar spinal cord enlargement, cervical and lumbar discs, paraspinal muscles in both regions of the spine and the gastrocnemius muscle since it is close to the region where behavioral sensitivity is measured in Task 3. Also, when available, we also harvested DRG samples but due to their small size it is not always possible. In the last year, we also broadened our assays to begin collecting leg bones, spinal facet joint and have also begun sampling blood serum for relevant biomarkers. We have focused on collecting tissue at several time points throughout the exposure, based on the behavioral outcomes observed for pain onset and/or resolution: day 1, day 7, day 8 and day 14. We also include a tissue from sham anesthesia groups at each time point. A complete summary of animal numbers (having the above listed tissues harvested) for each group to date is provided in Appendix A6. In addition, we are currently performing studies to generate tissues for day 14 from 8 Hz intermittent exposures and matched shams. These are currently underway and will be completed on October 30, 2013.

In the last report we detailed studies probing spinal cord and spinal discs at 7 days after the cessation of the repeated daily exposure. We do not re-describe those here, except to comment that findings have been presented or accepted for presentation at 3 national conferences and those abstracts are provided in Appendices A7-A9. In addition, we are preparing a manuscript reporting our finding of significant increases in neurotrophins in the cervical discs that will be submitted in the next few months. Please see Reportable Outcomes section for more specific details.

In the last year, we began analyzing the periaqueductal grey region of the brain for a variety of cellular receptors and transporters known to be involved in pain regulation. This work is ongoing, but the pilot studies with only 4 samples in each group are encouraging. Here, we provide those results to-date, along with quantification, supporting an increase in important regulators of the neurotransmiter

glutamate (GLT-1, EAAC1) both at day 1 and day 14 after the repeated vibration exposure compared to sham levels (Figure 14). These findings indicate that even a single vibration exposure at 15 Hz appears to be sufficient to induce an increase in these regulatory components. We continue to analyze these and other markers of brain activitiy in these models and to increase sample sizes. We will continue these studies over the next year.

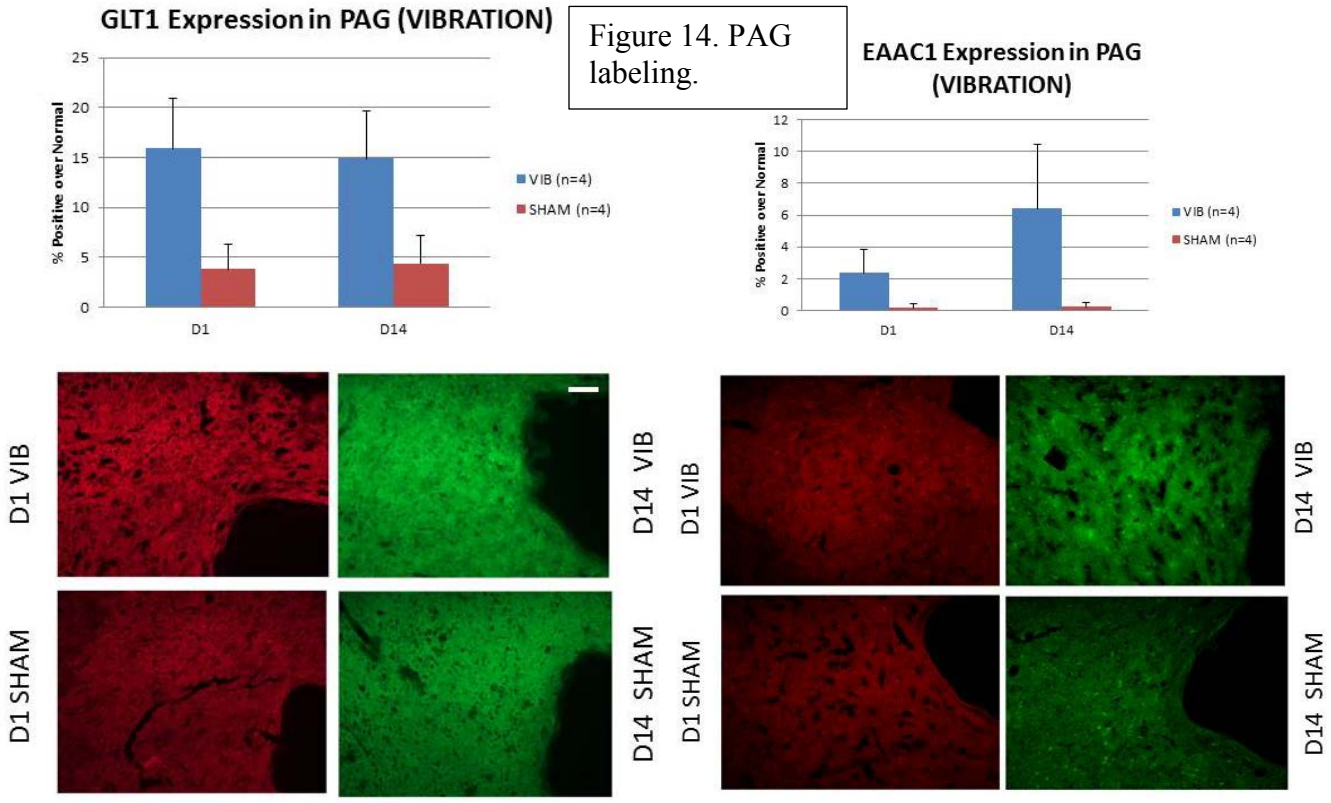


Figure 14. PAG labeling.

In the last year, we also continued our assays of the paraspinal and gastrocnemius muscles to evaluate if and to what extent muscle injury is induced by these vibration exposures. We broadened our investigations to include qPCR assays of genes of several inflammatory (TNF, thrombospondin, ITGAM) and neuro-regulatory proteins (CGRP, BDNF) and activated pathways (ERK) at day 1 after the a single vibration of 15 Hz (n=8) or sham exposure (n=2). Those studies indicate selective increases in innervation, neurotrophins and inflammation (Figure 15). Those findings led us to perform immunolabeling for a variety of related proteins, for which we now have methods in place – please see Appendix A10 for sample images.

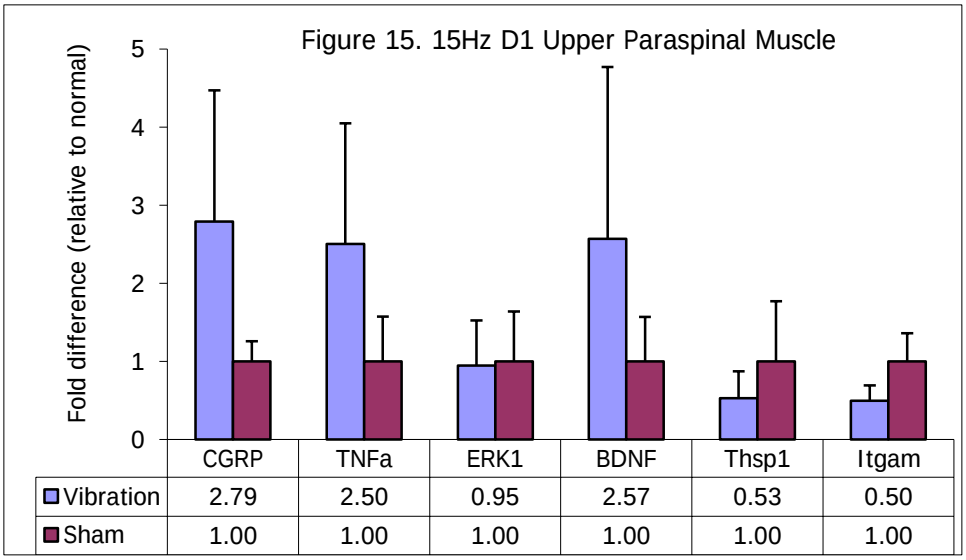

One particularly interesting labeling we have focused on is that of labeling for neuromuscular junctions (NMJ) (Figure 16; red labeling is NMJ, green is neuronal labeling). With those methods in place, we have recently quantified and compared the number of NMJs after a painful vibration exposure and pilot data suggest an immediate decrease as early as 1 day that is sustained until day 14 (Figure 17). However, additional studies with larger group sizes are needed. We are currently carrying out additional studies to increase group sizes and perform a more detailed investigation of these and other outcomes in the paraspinal and other muscles under this Task.

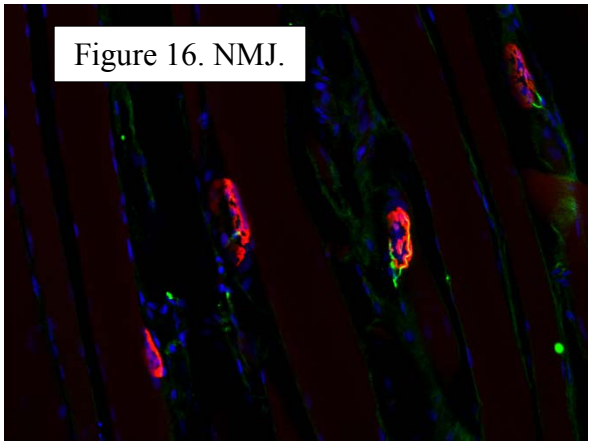

Figure 16. NMJ.

Recently, we have initiated studies to assess the effects of the 8 Hz vibration exposure on bone strength and structure. The bilateral femurs from three different groups will undergo imaging and mechanical testing: 8 Hz intermittent exposure with a stroke of 4.5 mm, 8 Hz intermittent exposure with a stroke of 1.5 mm, and sham. We have established protocols to perform microCT imaging to quantify cross-section, cortical thickness and volume, and trabecular bone volume and thickness. One leg from each rat will undergo such imaging followed by staining for Masson's Trichrome to look at osteoid seams. The other leg from each rat will undergo 3-point bending test to define its strength and stiffness. To date, we have harvested 7 sets of femurs from the 8 Hz exposure with a 4.5 mm stroke and are currently generating 4 pairs of shams and 3 pairs from 8 Hz with a 1.5 mm stroke – those will be harvested by 10/30/13. We also designed and fabricated a testing rig for these specimens and have established protocols for testing (Figures 18 & 19). These studies will be performed in November and December of 2013 and are expected to be submitted as a manuscript in Spring 2014.

Figure 17.

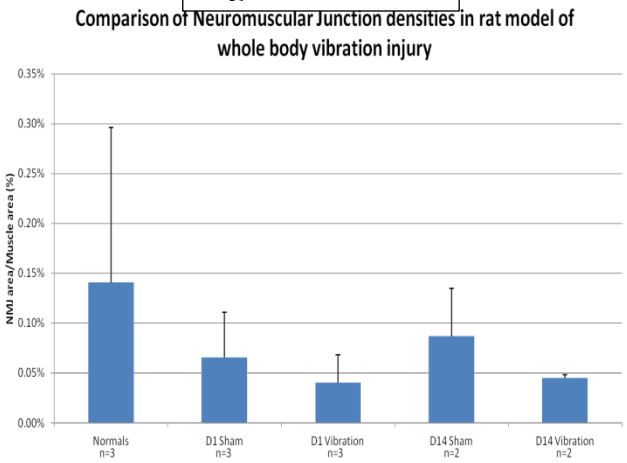


Figure 18. 3-pt bending set-up.

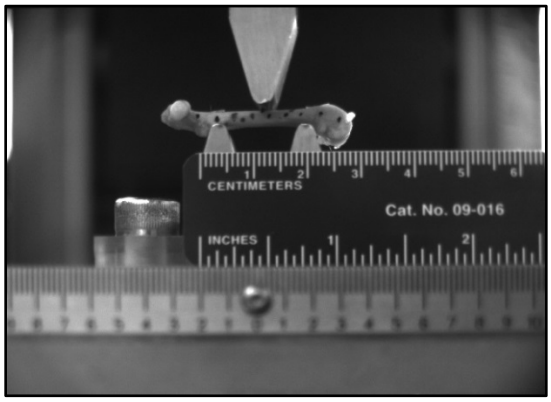


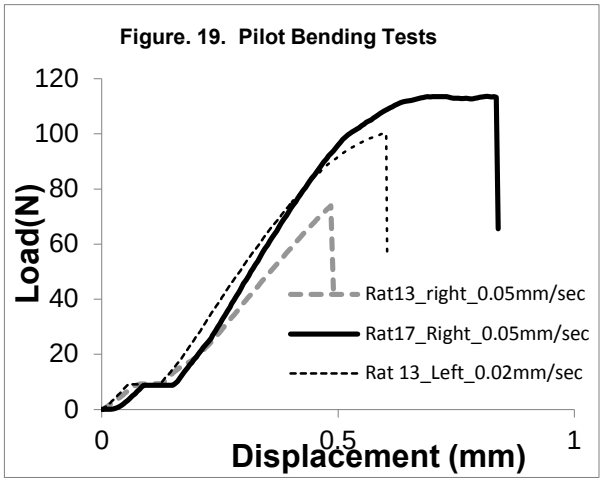

While our prior work focused last year on investigating the spinal discs (see above), in the last few months we have also turned attention to evaluating the spinal facet joints for evidence of injury, degeneration and/or ligament laxity. Here we present images providing evidence of our progress in establishing protocols to harvest, prepare and label facet joints in rat. The cervical spines from rats either in sham or undergoing the 15 Hz vibration were harvested, decalcified, axially section and stained with either Hematoxylin/Eosin (Figure 20, left) or with Masson's Trichrome (Figure 20, right). To date, we have generated tissues for these analyses and are initiating such evaluations, which will be performed over the next year.

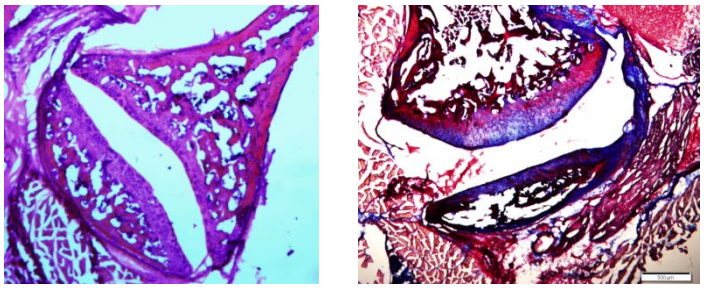

Figure 20. Facet joint labeling.

Lastly, in an effort to expand the utility of our models for providing a translational platform to detect injury and track health status we initiated studies to assay blood samples during the period after vibration exposures. Blood was drawn and processed to yield the serum from rats that had undergone the intermittent 8 Hz vibration (n=15) and from sham rats (n=3) at 4 time points during the course of the experiment: baseline (before the start of any experiments), at day 1, day 7 and day 14 from the start of the experiments. For each blood draw, rats were briefly anesthetized using inhalation isoflurane (4% induction, 3-4% maintenance) and the needle puncture site(s) on their tails was disinfected with alcohol wipes. Using a 23G needle and a 1 ml syringe, 100-300 uL of blood was collected from the rat tail artery. The first needle puncture was made at a site most distal on the rat tail where blood vessel was clearly visible. For subsequent blood draws for days 1 and 7 serum collection were made from sites proximal to the last site of needle puncture. For day 14, since the study was terminated on that day, blood was collected directly from a small incision made in the right atrium of the anesthetized rat (Nembutal, 65mg/Kg) prior to beginning perfusion with 1% PBS. The blood was transferred to sterile eppendorf tubes (1.5 ml), without additives allowed to clot at room temperature for 30- 40 minutes and centrifuged immediately at 1000g for 15 minutes at 4°C. The resulting supernatant was centrifuged again at 10,000g for 10 minutes at 4°C to produce a clear to yellowish-clear serum sample that was immediately frozen at -80°C until further analyzes. The concentrations of 23 cytokines were analyzed in the collected serum samples using a 96-well customized multiplex bead-based Luminex assay kit (Bio-Plex Pro rat Cytokine 23-plex Assay kit, Bio-Rad, Hercules, CA): EPO, G-CSF, GM-CSF, GRO/KC, IFN-γ, IL-1α, IL-1β, IL-2, IL-4, IL-5, IL-6, IL-7, IL-10, IL-12-p20, IL-13, IL-17, IL-18, M-CSF, MIP-3α, RANTES, TNF-α, VEGF and MCP-1. The samples were analyzed by researchers blinded to the study groups at the Human Immunology Core (HIC) a subsidiary of the Biomedical Research Core Facility of the University of Pennsylvania. All samples were analyzed as duplicates according to manufacturer's guidelines to decrease intra-assay variability. The samples were read on a special Luminex reader and cytokine serum concentrations were reported as pg/ ml serum. Serum cytokine levels analyzed at each day were compared to the matched levels at baseline for each rat using a Student's t-test.

Figure 21.

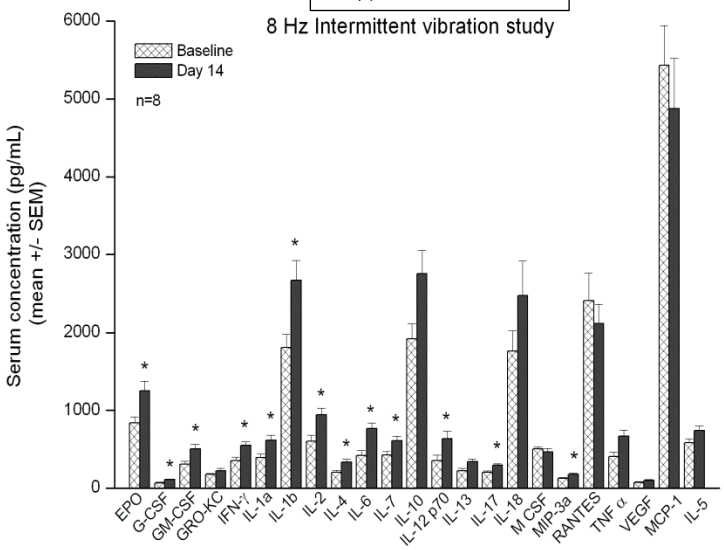


Serum concentrations of 20 of 23 tested cytokines trended towards an increase at day 1, day 7 and day 14 following the start of the experiment (Appendix A11). In particular, a total of 13 cytokines were significantly elevated serum levels at day 14 when compared to their baseline levels prior to any vibration (Figure 21): EPO (p=0.01), G-CSF (p=0.021), GM-CSF (p=0.042), IFN-γ (p=0.034), IL-1α (p=0.033), IL-1β (p=0.028), IL-2 (p=0.023), IL-4 (p=0.031), IL-6 (p=0.02), IL-7 (p=0.044), IL-12-p20 (p=0.046), IL-17 (p=0.019) and MIP-3α (p=0.042). At Day 7, serum cytokine levels of GRO/KC only was elevated when compared to baseline (Student's t-test, p= 0.043). At Day 1 the serum concentrations of none of the 23 cytokines tested were significantly changed when compared to the baseline values.

As mentioned above, additional studies at different relevant time points are ***ongoing*** and are ***planned*** for the remainder of the project period. However, based on the data already gathered from several of these assays, we anticipate submitting several manuscripts – particularly detailing the brain, serum and leg bone findings – in the next 6 months. We will continue to integrate the tissue results with those of the biomechanical data to complete **Task 4e** in the next year.

**Task 5**

Work under **Task 5** corresponds to identification of publications for work from Aims 2 and 3 and has been completed in part but is also ongoing. It will be completed by the end of Year 4 as detailed in the original statement of work. To date under the entire project period, we have presented 10 abstracts, published 1 paper, submitted 2 other manuscripts, and are currently preparing 2 manuscripts, both of which will be submitted in the next 3 months. Please see Appendices A1, A2, A4, A7-A9 for the abstracts and manuscript that have been presented, published or accepted during Year 3. Please also see the Reportable Outcomes section for additional details.

**Task 6**

Work under **Task 6** corresponds to Aim 4 which broadly consists of efforts to provide the model system and software as resources for the broader scientific community. The majority of the specific sub-tasks of that Aim are largely planned for the remaining year of this project. However, given our early successes in developing a working system and identifying the conditions for use in Aims 2 and 3, we also continue with **Task 6a** and **Task 6c**. We continue these analyses and are investigating more economic options for components of our device. In fact, in the last year we implemented a new programmable shaker in our device which has improved performance capabilities compared to the motor of our first-generation device (see **Task 3**). Further, that component is far more affordable ($3,865.50). Because of this work under **Task 6b** to seek additional funding was not needed. We will continue these ***ongoing*** efforts over the next year. Work in **Task 6c** has been completed through our scaling studies between the rat (from our μCT) and human (from literature) in Aim 2. Efforts under **Task 6c** are ongoing and will continue as originally projected to be completed before or by the end of Year 4. All **other sub-tasks of Task 6** are planned for completion by the end of Year 4, according to the original timeline.

## KEY RESEARCH ACCOMPLISHMENTS

- Determined the resonant frequency of the rat spine to be 8 Hz and for the human spine to be 4 Hz for vibration along the long-axis of the spine.
- Determined the muscle activation response to vibration in the human and compared to spinal transmissibility response
- Derived complete anatomic datasets quantifying the bony anatomy of the rat cervical and lumbar spines for direct comparison (and scaling) to the human spine.
- Developed a lumped parameter mathematical model of the rat spine and performed validation studies that indicate these simple models are fairly good at capturing the rat response.
- Established several different exposure profiles that impose sustained and transient pain, for single and repeated exposure respectively, in the live rat.
- Determined several changes in tissue responses (spinal cord, disc, muscle, brain) in association with sustained pain.
- Established methodology to enable assays of leg bone strength and structure using μCT techniques and developed a working protocol for such studies.
- Established protocols for evaluating facet joint health and structure after vibration exposure.
- Established protocols to assay blood serum levels of cytokines and performed pilot studies on those biomarkers.

## REPORTABLE OUTCOMES

***Manuscripts, Abstracts & Presentations during Year 3***

1. Baig HA, Guarino BB, Lipschutz DE, Winkelstein BA. Whole body vibration induces forepaw and hind paw behavioral hypersensitivity in the rat. *Journal of Orthopedic Research*, 31(11):1739-1744, 2013.
2. Baig HA, Dorman DB, Shivers BL, Chancey VC, Winkelstein BA. Characterization of the frequency & muscle responses of the lumbar and thoracic spines of seated volunteers during sinusoidal whole body vibration. *Journal of Biomechanical Engineering,* submitted.
3. Jaumard NV, Baig HA, Zhang S, Zhou T, Lee J, Guarino BB, Winkelstein BA. A lumped parameter model of axial whole body vibration in the rat. *Journal of Biomechanics*, submitted.
4. Kartha S, Zeeman M, Guarino BB, Baig HA, Winkelstein BA. Painful vibration along the spine induces increased expression of neurotrophins in the cervical discs in a rat model. *To be submitted*.
5. Jaumard NV, Leung J, Gokhale AJ, Guarino BB, Winkelstein BA. The rat spine is an appropriate surrogate for human spinal biomechanical studies. *To be submitted*.
6. Tanaka K, Baig HA, Guarino BB, Smith JR, Winkelstein BA, Jordan-Scuitto KL. Painful Whole Body Vibration is Associated with Decreased BiP Expression in the Lumbar Spinal Cord. *American Association of Endodontics Annual Session*, #OR12, Honolulu, HI, March 2013.
7. Baig HA, Dorman DB, Shivers BL, Breaux-Waltz A, Chancey VC, Winkelstein BA. Characterization of the Frequency & Muscle Response in the Lumbar & Thoracic Spines during Sinusoidal Vertical Whole Body Vibration. *ASME Summer Bioengineering*

*Conference*, #SBC2013-14055, Sunriver, OR, June 2013. (3rd place winner in student paper competition at conference).

8. Jaumard NV, Baig HA, Guarino BB, Winkelstein BA. A Three Degree of Freedom Lumped Parameter Model of Whole Body Vibration Along the Spine in the Rat. *ASME Summer Bioengineering Conference*, #SBC2013-14111, Sunriver, OR, June 2013.
9. Zeeman ME, Kartha S, Baig HA, Guarino BB, Winkelstein BA. Painful Whole Body Vibration Induces Increased Expression of Nerve Growth Factor & Brain-Derived Neurotrophic Factor in Cervical Intervertebral Discs in a Rat Model. *Society for Neuroscience*, #267.05/UU20, San Diego, November 2013.
10. Kartha S, Zeeman ME, Baig HA, Guarino BB, Winkelstein BA. Upregulation of NGF & BDNF in Cervical Intervertebral Discs Exposed to Painful Whole Body Vibration. *2nd International Philadelphia Spine Research Symposium*, Philadelphia, PA, November 2013, accepted.

***Degrees Obtained Supported by this Award***

1. Akhilesh Gohkale, MSE in Mechanical Engineering and Applied Mathematics, awarded 2012
2. Nadia Garbhi, MS in the Dental School, awarded 2013.
3. Hassam Baig, currently an MSE student in Bioengineering, degree expected in December 2013.
4. Kosuke Tanaka, currently an MS student in the Dental School, degree expected in 2014.
5. Ben Freedman, PhD student did a research rotation working on this project in Fall 2011.
6. Lorre Atlan, PhD student did a research rotation working on this project in Fall 2011.
7. Sijia Zhang, PhD student did a research rotation working on this project in Fall 2012.
8. Ben Bulka, PhD student currently doing a research rotation (Fall 2013) working on this project.

***Animal Model Generated***

1. Protocol developed to induce sustained behavioral sensitivity following repeated daily vibration to the rat.
2. Protocol developed to induce transient behavioral sensitivity following a single vibration to the rat.
3. Protocol developed to induce sustained behavioral sensitivity following a single vibration exposure to the rat.

***Research Opportunities Applied for or Received Supported by this Award***

1. DURIP proposal awarded July 2013, for high rate tissue tester to ext4end activities under this award, application pending.

## CONCLUSIONS

There is currently very little definitive mechanistic data defining the relationships between whole body or spine vibration, tissue responses (biomechanical and physiological) and pain. Considering that pain is a tremendous problem especially for the military personnel, we have developed a useful model platform to study how such exposures produce and modulate pain. We **hypothesized** that a model of vibration and/or jolt induced pain could be produced in the rat that would simulate the human exposures. **Studies performed in the last year (in addition to those reported in our prior progress reports) continue to support our hypothesis and have importance in moving the entire project forward**. Among the major findings of importance include the fact that even 30 minutes of vibration a day for even 1 day, at a certain frequency related to the resonance frequency, is sufficient to induce significant widespread behavioral sensitivity that is sustained for two weeks. A second major important finding is that there are also widespread physiologic modifications in tissues and biomarkers that correspond to that response. Indeed, these behavioral findings have the ***very important implication that rest periods must be adequately long between even repeated single exposures to prevent the development and maintenance of pain and/or injury***.

In addition, we have also found that a host of biochemical changes appear to be present in association with pain and are evident in the periphery and central nervous system. Interestingly, while the resonant frequency of the rat is at 8 Hz, the human spine resonates at ~4 Hz. This has important implications as we proceed with scaling our findings to the human. But it must also be noted that this difference may be due to the experimental set-ups of the two species with the rat in the prone position and the human seated. Interestingly, the muscle activation response of the human corresponds to its resonance frequency, and the resonance frequency of the rat produces more robust pain behaviors. We continue to integrate human, rat and mathematical models together in this project in order to fully-define the consequences of vibration from a mechanical, functional and physiological perspective**.**

Based on the activities during the last year, we do not have any modifications to the future work, only to recommend slight changes to the proposed activities related to the MARS studies. As indicated above, we were initially substantially delayed in getting regulatory approval for those activities to analyze data from USAARL in Aim 1 (Task 2). We made tremendous progress in the last year to analyze in great depth the prior datasets and in working with those datasets, it is clear there is even more data that can still be analyzed to provide valuable insights about the human response to vibration. Given the remaining Tasks in the next year, we believe our efforts are best spent further understanding the relationships between the biomechanics, spine responses, tissue responses and pain – and that continued work to define potential biomarkers for injury and/or pain will provide more meaningful translational impact for the military population. We believe we are currently positioned to move that work forward in an effective and meaningful way. In fact, those data may provide great context for establishing more meaningful risk assessment algorithms for pain and injury, since the current ones rely largely on speculative notions and standards for injuries that may not be relevant.

Accordingly**,** our in vivo model that mimics the biomechanical loading to the body enables studying how loading produces tissue injury, which tissues are injured, how pain develops, and which conditions place the military specialists at greatest risk for injury. The new knowledge gained from such an injury/pain model has direct utility for evaluating injury risks and developing potential rest-period strategies to prevent injury and alleviate pain. Our findings to date already provide evidence that even low level vibration is sufficient to produce pain and that even a single exposure in some cases, and a rest period that is long enough for symptoms to resolve in other cases, is not sufficient to prevent the subsequent maintenance of symptoms or development of symptoms upon re-exposure. Our in vivo and mathematical models, along with our assays of physiologic function that have already been developed under this project have tremendous promise for providing major benefit to the military by identifying tissues at risk for injury and exposures which pose the greatest threats to producing pain.

## REFERENCES


1. Baig HA, Dorman DB, Shivers BL, Chancey VC, Winkelstein BA, 2013, Characterization of the frequency & muscle responses of the lumbar and thoracic spines of seated volunteers during sinusoidal whole body vibration. *J Biomech Eng,* submitted.

2. Nevin R, Means G, 2009, Pain & discomfort in deployed helicopter aviators wearing body armor. *Aviat Space Environ Med*, 80: 807-810.

3. Heino M, Ketola R, Makela P, Makinen R, Niemela R, Starak J, Partanen T, 1978, Work conditions and health of locomotive engineers. *Scandinavian Journal of Work Environment & Health*, 4: 3-14.

4. Griffin MJ, 1978, The evaluation of vehicle vibration and seats. *Applied Ergonomics*, 9.1: 15-21.

5. Panjabi MM, Andersson GJ, Jorenus L, 1986, In vivo measurements of spinal column vibrations. *Journal of Bone & Joint Surgery*, 68: 695-702.

6. Mansfield NJ, Griffin MJ, 2000, Non-linearities in apparent mass and transmissibility during exposure to whole-body vertical vibration. *J Biomechanics*, 33: 933-41.

7. Smith SD, Kazarian LE, 1994, The effects of acceleration on the mechanical impedance response of a primate model exposed to sinusoidal vibration. *Ann Biomed Eng*, 22: 78-87.

8. Holmlund P, Lundstrom R, 2001, Mechanical impedance of the sitting human body in single-axis compared to multi-axis whole-body vibration exposure. *Clinical Biomechanics*, 16: S101-S110.

9. Nawayesh N, Griffin MJ, 2005, Non-linear dual-axis biodynamic response to fore-and-aft whole body vibration. *Journal of Sound & Vibration*, 282: 831-862.

10. Cameron B, Morrison J, Robinson D, Vukusic GA, Martin S, Roddan G, Albano JP, 1996, "Development of a standard for the health hazard assessment of mechanical shock and repeated impact in Army vehicles – Phase 4," USAARL Contract Report No. CR-96-1, Fort Rucker, AL.

11. Alem N, Hiltz E, Breaux-Sims A, Bumgardner B, 2004, Evaluation of new methodology for health hazard assessment of repeated shock in military tactical ground vehicles. NATO RTO-Applied Vehicle Technology Symposium, Prague, Czech Republic, October 2004, RTO-AVT-110, Paper 7, pp 1-18.

12. Baig HA, Guarino BB, Lipschutz DE, Winkelstein BA, 2013, Whole body vibration induces forepaw and hind paw behavioral hypersensitivity in the rat. *J Orthopedic Res*, 31(11):1739-1744.

13. Nicoll SB, Hee CK, Davis MB, Winkelstein BA, 2010, A rat model of TMJ pain with histopathologic modifications. *J Orofacial Pain*, 24(3): 298-304.

# APPENDIX

**A1.** Poster presented at ASME Mtg. in June, 2013.

## Characterization of the Frequency & Muscle Responses in the Lumbar & Thoracic Spines During Sinusoidal Vertical Whole Body Vibration

Hassam A. Baig[1], Daniel B. Dorman[2], Bethany L. Shivers[2], Arlene Breaux-Waltz[2], V. Carol Chancey[2], Beth A. Winkelstein[1]
[1]Department of Bioengineering, University of Pennsylvania, Philadelphia, PA & [2]US Army Aeromedical Research Laboratory, Fort Rucker, AL

### Introduction

- Operators of off-road vehicles, industrial trucks, tractors, and buses, and helicopter pilots are exposed to repeated whole body vibration (WBV) [1,2]. WBV has been linked to chronic neck and lower back pain [1,2].
- The cyclic muscle response to WBV has been suggested to lead to muscle fatigue, a mechanism that can further contribute to the development of low back pain [3].
- Although several studies have measured the transmissibility response of the human spine [4,5], studies defining the mechanical effects of whole body vibration in a seated human are limited [4,5] and none has investigated the relationship between the biomechanical and muscle activity responses during such WBV exposures.

**Study Objective:** The goals of this study were to (1) characterize the frequency response of seated human volunteers during WBV exposures along the vertical axis of the spine in order to define the resonant frequency in the lumbar and thoracic spines, and (2) use electromyography (EMG) to measure muscle activity at both spinal regions in order to compare the corresponding muscle and resonant responses for varied input WBV frequencies in the human.

### Methods

**Experimental Setup:**

- Under USAMRMC IRB-approved procedures, 5 male volunteers (24.8±2.2 years; 73.9±7.3 kg; standing height 1.8±0.1 m) underwent seated WBV [6].
- Each vibration exposure included a sine sweep ranging from 2-19Hz, with a 0.4g amplitude, for a total exposure time of 70 seconds.
- Accelerometers and infrared emitting diodes were mounted on the seat pad and attached to the subject's skin over the lumbar (L4, L5) and thoracic (T3, T4) spinal regions (Fig. 1).

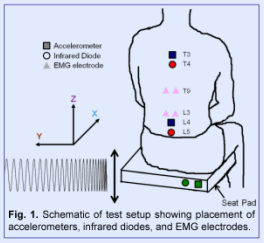


**Fig. 1.** Schematic of test setup showing placement of accelerometers, infrared diodes, and EMG electrodes.

- EMG activity was measured using surface electrodes placed over the lumbar (L3) and thoracic (T9) paraspinal muscles (Fig. 1).
- Acceleration and EMG data were acquired at 500Hz and image data were acquired at 200Hz throughout the entire 70 second exposure for each subject.

**Data Analysis:**

- Accelerometer, image, and EMG signals were segmented into 35 2-second epochs.
- Frequency was calculated using spectral analysis in MATLAB.
- Maximum voluntary contraction (MVC) was measured using EMG prior to vibration for each subject.
- Transmissibility and the muscle response (MR) were calculated using standard equations [7,8] (Fig. 2).
- EMG data from the left and right sides were averaged for muscle response analysis.

$$\text{Transmissibility} = \frac{\text{RMS Spinal Acceleration}}{\text{RMS Seat Acceleration}}$$

$$\text{Muscle Response} = \frac{\text{RMS EMG}}{\text{Maximum Voluntary Contraction}}$$

**Fig. 2.** Equations used to calculate transmissibility and muscle response (MR).

### Results

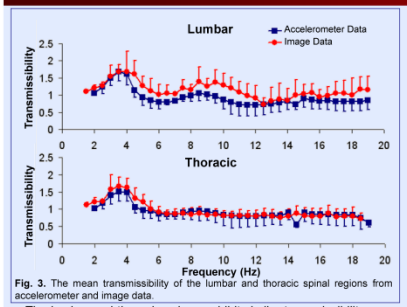


**Fig. 3.** The mean transmissibility of the lumbar and thoracic spinal regions from accelerometer and image data.

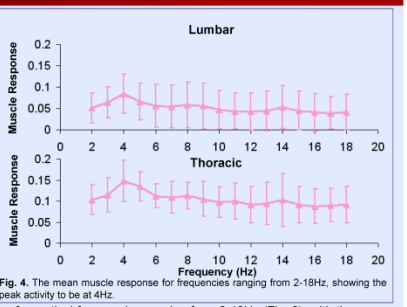


**Fig. 4.** The mean muscle response for frequencies ranging from 2-18Hz, showing the peak activity to be at 4Hz.

- The lumbar and thoracic spines exhibit similar transmissibility responses for vertical frequencies ranging from 2-19Hz (Fig. 3), with the same resonant frequency (4Hz) in both regions of the spine.
- A possible second dominant frequency is evident in the lumbar spine between 8-10Hz (Fig. 3) and is similar whether determined by methods using accelerometer-based or image-based data (Fig. 3).
- The peak MR is detected at 4Hz (Fig. 4); this is the case for the muscles in both the lumbar and thoracic regions of the spine (Fig. 4).
- The MR exhibits nearly identical response patterns in the lumbar and thoracic spinal regions over the frequency ranges in this study (Fig. 4).

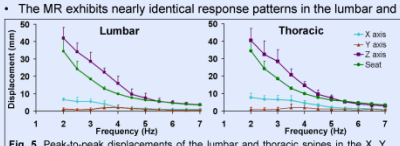


**Fig. 5.** Peak-to-peak displacements of the lumbar and thoracic spines in the X, Y, and Z directions and the seat pad for frequencies ranging from 2-7Hz.

- Peak-to-peak displacements along all three axes were calculated using the imaging markers (Fig. 1) for frequencies within the range (2-7Hz) around the resonant peak (Fig. 3).
- Vertical displacement of the seat and Z-direction of the humans follow a similar pattern in both spinal regions, but show greater difference in the thoracic region (Fig. 5).
- The dominant motion is the Z-direction (Fig. 5), suggesting the increased muscle activation at these frequencies is caused by motion along the long-axis of the spine.

### Discussion

- The resonant frequency (4Hz) for the seated volunteer in this study (Fig. 3) is comparable to other reports for the lumbar spine, in which the resonance in the vertical direction has been reported to be in the range of 4-6Hz, with a second resonance at 8-10Hz [4,5].
- Interestingly, the peak muscle response in both spinal regions also occurs at this primary resonant frequency (Figs. 3 & 4). Although muscle activity on the left and right sides was not differentiated, the evoked muscle activity for each subject was normalized to MVC (Fig. 2) for each subject, which accommodates any differences that may exist for individuals, such as muscle strength.
- Although muscle fatigue and pain were not assessed, increases in muscle activity observed at the resonant frequency (Figs. 3 & 4) suggests a possible mechanism by which muscle fatigue may be more likely (or even more severe) and may lead to the development of pain [3].
- Continued studies incorporating other physiological outcomes and more complex loading scenarios may provide important insight into the pathobiomechanical mechanisms of this type of common painful injury. Changes in pain-related neuropeptides and pain have been reported in animal models of WBV at the corresponding resonant frequencies [7,9,10]. Future work, coordinating animal and human biomechanical studies, that also integrates neurophysiological assays may improve our understanding of WBV injury and the relationship between WBV, tissue biomechanics and physiological responses.

### References

**[1]** Boshuizen H et al. (1999) *Spine*, 24, 2506-15; **[2]** Nevin R et al. (2009) *Aviat Space Environ Med*, 80, 807-10; **[3]** Bongers P et al. (1990) *Ergonomics*, 33, 1007-26; **[4]** Panjabi M et al. (1986) *J Bone & Joint Surg*, 68, 695-702; **[5]** Mansfield N & Griffin M. (2000) *J Biomech*, 33, 933-41; **[6]** Cameron B et al. (1996) *USAARL Report No. CR-96-1*; **[7]** Baig H et al. (2012) *NEBEC Ann Mtg*; **[8]** Wirth B et al. (2011) *J Electromyography & Kinesiology*, 21, 450-7; **[9]** Weinstein J et al. (1988) *Spine*, 13, 521-5; **[10]** Baig H et al. (2013) *J Orthop Res*, in press.

### Acknowledgements

Funding provided by a DOD-CDMRP (W81XWH-10-2-0140) grant and USAARL. The views, opinions, and/or findings in this poster are those of the authors and should not be construed as an official Department of the Army position, policy, or decision, unless so designated by other official documentation. Citation of trade names does not constitute an official Department of the Army endorsement or approval of the use of such commercial items.

**A2.** Reprint of manuscript published in *Journal of Orthopaedic Research*, 2013.

See following pages

# Whole Body Vibration Induces Forepaw and Hind Paw Behavioral Sensitivity in the Rat

**Hassam A. Baig, Benjamin B. Guarino, Daniel Lipschutz, Beth A. Winkelstein**

Department of Bioengineering, University of Pennsylvania, 240 Skirkanich Hall, 210 S. 33rd Street, Philadelphia, PA, 19104-6321

*Received 20 December 2012; accepted 13 June 2013*
*Published online 7 July 2013 in Wiley Online Library (wileyonlinelibrary.com). DOI 10.1002/jor.22432*

**ABSTRACT:** Whole body vibration (WBV) has been linked to neck and back pain, but the biomechanical and physiological mechanisms responsible for its development and maintenance are unknown. A rodent model of WBV was developed in which rats were exposed to different WBV paradigms, either daily for 7 consecutive days (repeated WBV) or two single exposures at Day 0 and 7 (intermittent WBV). Each WBV session lasted for 30 min and was imposed at a frequency of 15 Hz and RMS platform acceleration of 0.56 ± 0.07 g. Changes in the withdrawal response of the forepaw and hind paw were measured, and were used to characterize the onset and maintenance of behavioral sensitivity. Accelerations and displacements of the rat and deformations in the cervical and lumbar spines were measured during WBV to provide mechanical context for the exposures. A decrease in withdrawal threshold was induced at 1 day after the first exposure in both the hind paw and forepaw. Repeated WBV exhibited a sustained reduction in withdrawal threshold in both paws and intermittent WBV induced a sustained response only in the forepaw. Cervical deformations were significantly elevated which may explain the more robust forepaw response. Findings suggest that a WBV exposure leads to behavioral sensitivity. © 2013 Orthopaedic Research Society. Published by Wiley Periodicals, Inc. J Orthop Res 31:1739–1744, 2013

**Keywords:** whole body vibration; spine; pain; injury

Several epidemiological studies have linked exposure to whole body vibration (WBV) with neck and back pain,[1–4] suggesting that vibration can lead to the onset of both pain syndromes. American male workers operating vibrating vehicles, such as industrial trucks and tractors, have been reported to have a higher prevalence of low back pain and are three-times more susceptible to acute herniated lumbar discs than workers whose occupations do not involve such exposures.[3,5] Also, military helicopter aviators report increased pain during deployment compared to their pre-deployment reports of pain, with between 22–37% reporting neck and 39–70% reporting low back pain.[4] Further, the frequency of pain was significantly higher for aviators who experienced substantially increased flight hours during deployment compared to those who did not,[4] suggesting that the amount of exposure to WBV may affect the pain.[4] Despite the strong suggestive evidence of these epidemiological studies that pain can develop from WBV and may be influenced by the nature and frequency of the exposure, there is still little known about how these factors relate to the onset, maintenance, and resolution of pain.

A limited number of studies have defined the biomechanical response to vibration and related resonance and vibration frequency to physiological responses known to be involved in pain-related injuries. The resonant frequency of the seated human undergoing vertical vibration has been reported to be 4.5 Hz from a series of studies using accelerometers on the first and third lumbar vertebrae (L1, L3) and the sacrum of volunteers exposed to vertical vibrations, ranging in frequencies from 2 to 15 Hz.[6] A later study using similarly seated human volunteers, with accelerometers placed on L3 and vertical vibration frequencies ranging from 0.2 to 20 Hz with varying magnitudes also reported a primary resonance of 4–6 Hz, with a secondary resonance between 8 and 12 Hz.[7] Interestingly, the resonant frequency of the prone rabbit exposed to horizontal vibration between 2 and 8 Hz also was approximately 4.5 Hz.[8] In contrast, the resonance of the seated primate in the vertical direction ranges from 9 to 15 Hz.[9] In addition to these biomechanical studies, studies have reported changes in pain-related neuropeptides and damage to arterial endothelial cells for WBV exposures ranging from 4.5 to 60 Hz.[8,10] Although all of these studies suggest WBV as a putative mechanism to induce pain and provide important mechanical and physiological context for that hypothesis, the relationship between WBV and pain still remains speculative.

The objective of this study was to develop an in vivo model of WBV in the rat, and to evaluate pain responses for two different vibration exposure paradigms, investigating the relative effects of an only intermittent exposure and a repeated daily exposure. Based on prior transmissibility studies,[7–10] each WBV exposure was applied at a frequency of 15 Hz for 30 min. The effect of each WBV exposure was measured in the context of the onset and/or maintenance of behavioral sensitivity, using alterations in the paw withdrawal responses for the forepaw and hind paw. To provide mechanical and anatomical regional context for behavioral responses between exposure groups, the deformations in the cervical and lumbar regions of the rat during each WBV exposure were also measured to quantify the compression and extension in each region.

## METHODS

All procedures were approved by the University of Pennsylvania the Institutional Animal Care and Use

Grant sponsor: Department of Defense; Grant number: W81XWH-10-2-0140.
*Correspondence to*: Beth A. Winkelstein (T: 215-573-4589; F: 215-573-2071; E-mail: winkelst@seas.upenn.edu)

Committee and performed in accordance with the Committee for Research and Ethical Issues of the International Association for the Study of Pain.[11] Experiments were performed using male Holtzman rats (weighing 280–360 g at the start of the study), housed under conditions approved by the United States Department of Agriculture and the Association for Assessment and Accreditation of Laboratory Animal Care International, with a 12–12 h light–dark cycle and free access to food and water.

Vibration exposure was performed under inhalation anesthesia (4% isoflurane for induction, 3.5% for maintenance). Separate groups of rats underwent a whole body vibration either daily for 7 consecutive days starting on Day 0 (*repeated WBV*; $n = 6$) or two single exposures of vibration at Day 0 and again on Day 7 (*intermittent WBV*; $n = 8$; Fig. 1). A control group (*sham*; $n = 4$) underwent anesthesia exposure according to the timing and scheduling used in the *repeated WBV* group (Fig. 1). For each session of vibration exposure, after anesthesia was induced the rat was placed in the prone position on an acrylic platform that was vibrated in the horizontal ($x-$) direction at 15 Hz, with a peak-to-peak magnitude of 1.5 mm for 30 min, secured to the platform by velcro straps (Fig. 2). The platform was rigidly fixed to a linear servomotor (MX80L; Parker Hannefin; Cleveland, OH) controlled by a digital driver (VIX500IH; Parker Hannefin). A laser displacement sensor (LTC-050-10; MTI; 1.25 μm/mV) tracked the platform motion. Two miniature quartz shear accelerometers (ACC104A; Omega; 10 mV/G) measured the acceleration of each of the plate and the rat: one accelerometer was affixed to the moving plate and the other was embedded in a velcro strap secured to the lumbar region of the rat (Fig. 2). During WBV, black ink markings on the platform, the lumbar accelerometer, the lumbar velcro strap, and the stationary stage, as well as the eye itself, were tracked using a high speed CCD camera (VRI-MIROEX1-1024MM; Phantom; $640 \times 480$), to measure their respective displacements during each exposure session on Days 1 and 7 (Figs. 1 and 2). Accelerometer, imaging, and displacement data were each recorded at 120 Hz.

The accelerations and displacements of the plate and the rat were measured during WBV using the accelerometers and image markers in order to verify

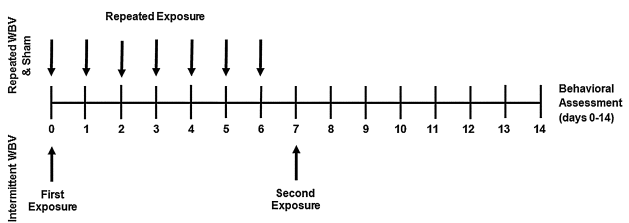


**Figure 1.** Schematic illustrating the timeline for exposures, rest periods, and daily behavioral assessment for the *repeated WBV*, *sham*, and *intermittent WBV* groups.

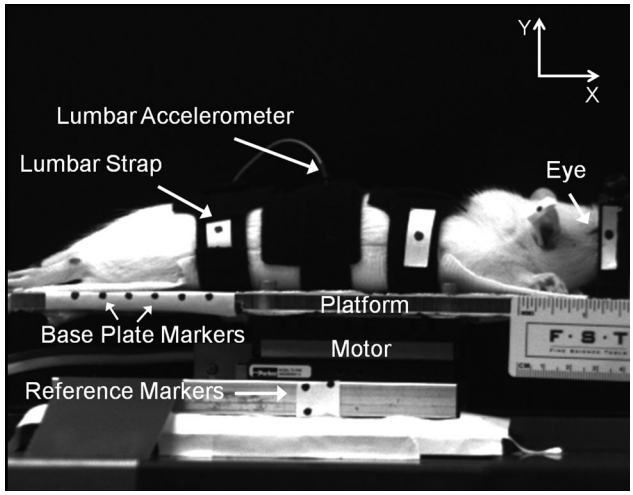


**Figure 2.** Image of the experimental setup showing the base plate, motor, lumbar accelerometer, and markers on the rat. The $x-$ (horizontal) and $y-$ (vertical) directions are also indicated.

that equivalent exposures were imposed and that similar kinematics were induced in the different groups. For each exposure, 15 min of the accelerometer data were used to determine the root mean square (RMS) acceleration for each of the plate and the rat, which were then averaged over all days of exposure for each rat. Similarly, 12 s of image data were taken to determine the displacements of the plate, the rat, the lumbar segment, and the eye (as a marker for the head), by digitizing their positions relative to the stationary reference markers in each image using ProAnalyst (Xcitex, Inc.; Cambridge, MA) (Fig. 2). Both sets of data were filtered using a 5th order Butterworth bandwidth filter. For each exposure, 15 min of displacement data were used to determine the mean peak-to-peak plate displacements, which were averaged over all exposure days for each rat. A repeated-measures ANOVA compared displacements and accelerations over the different exposure days and a one-way ANOVA compared the plate displacements and rat accelerations between groups.

The local two-dimensional deformations in each of the cervical and lumbar regions were determined in the sagittal plane (Fig. 2) during each WBV session using image data in order to estimate the extent of compression and/or extension. To do so, the vector lengths of the cervical region, taken between markers on the eye and the lumbar accelerometer, and of the lumbar region, defined between the lumbar accelerometer and the lumbar strap, were separately determined using the digitized positions from the images. The resting vector length for each region was defined as the length of the vector in the initial frame of the images, prior to any vibration. The maximum and minimum vector lengths also were calculated for each cycle of the WBV and the average maximum and minimum lengths were subtracted from the corresponding resting length for each rat to calculate the

change in vector length for each rat, separately for the cervical and the lumbar region. The accuracy in identifying and tracking the markers is $0.035 \pm 0.054$ mm. The error in measuring these vector lengths in this way is also small: $0.079 \pm 0.046$ mm for maximum vector length and $0.079 \pm 0.039$ mm for minimum vector length. Separate paired Student's *t*-test compared the change in lengths for the cervical and lumbar lengths.

Behavioral sensitivity was assessed by measuring the threshold for withdrawal in the bilateral forepaws and hind paws on all days in order to quantify the onset and maintenance of increased tactile sensitivity after procedures. Prior to any vibration exposure, rats were also assessed to provide a baseline measurement to serve as an unexposed control response for each rat. Methods to measure the paw withdrawal threshold were adapted from Chaplan's up/down method and have been previously reported and validated.[12–14] The response threshold was measured using increasing strengths of von Frey filaments (0.6, 1.4, 2.0, 4.0, 6.0, 8.0, 10.0, 15.0, and 26.0 g-force), applied to the plantar surface of each paw. The lowest-strength filament to provoke a positive withdrawal response was taken as the response threshold if a positive withdrawal response was also validated by application of the next higher filament. Each testing session consisted of three rounds of five stimulations to each forepaw and hind paw, with at least a 10-min rest period separating each round. The positive responses of each rat for each of three rounds were recorded and averaged. The average forepaw and hind paw responses were separately averaged by group on each testing day. A repeated-measures ANOVA with Bonferroni correction compared temporal withdrawal thresholds between the *repeated WBV*, *intermittent WBV*, and *sham* groups. For the *intermittent WBV* group, a rate of recovery for each rat after an exposure was determined by calculating the best-fit line of the average withdrawal response, fitting the data after the first (Days 1–7) and second (Days 8–14) exposures (Fig. 1), separately for the forepaw and hind paw. A one-way ANOVA compared the rate of recovery between the two exposures for each of the paws, separately.

## RESULTS

All rats demonstrated normal functioning with grooming and weight gain consistent with normal rats. The mean weight gain over the study period was $75 \pm 18$ g for the *repeated WBV* group, $97 \pm 14$ g for the *intermittent WBV* group, and $86 \pm 25$ g for the *sham* group, and was not different between groups. Rats that underwent either of the vibration exposure types showed normal mobility, with no adverse effects of the procedure.

Both the repeated and intermittent vibration groups were exposed to the same vibration profiles of the base plate. The mean RMS acceleration of the plate in the *repeated WBV* group was $5.79 \pm 0.70$ m/s$^2$ and $5.32 \pm 0.67$ m/s$^2$ in the *intermittent WBV* group, and was not significantly different from each other (Table 1). The mean horizontal displacement of the base plate also was not different between these two exposure groups: $1.93 \pm 0.46$ mm for the *repeated WBV* and $1.45 \pm 0.25$ mm for the *intermittent WBV* groups (Table 1). The mean RMS acceleration of the rats in the *repeated WBV* group was $6.18 \pm 0.69$ m/s$^2$ and $6.16 \pm 1.01$ m/s$^2$ in the *intermittent WBV* group (Table 1). Neither the acceleration of the plate nor the rat was significantly different between the two injury groups.

**Table 1.** Summary of Measured Accelerations and Displacements During Repeated and Intermittent WBV

| WBV Group | Rat ID | Plate RMS Acceleration (m/s$^2$) ± SD | Rat RMS Acceleration (m/s$^2$) ± SD | Plate Displacement (mm) ± SD |
|---|---|---|---|---|
| Repeated WBV | 1 | 6.26 ± 0.49 | 6.83 ± 0.34 | 2.24 ± 0.28 |
| | 2 | 6.28 ± 0.51 | 6.68 ± 0.07 | 2.23 ± 0.13 |
| | 3 | 6.34 ± 0.51 | 6.67 ± 0.18 | 2.49 ± 0.09 |
| | 4 | 6.08 ± 0.57 | 6.25 ± 0.68 | 1.82 ± 0.14 |
| | 12 | 4.87 ± 0.41 | 5.53 ± 1.14 | 1.40 ± 0.07 |
| | 13 | 4.93 ± 0.41 | 5.15 ± 0.73 | 1.42 ± 0.12 |
| Repeated WBV, mean ± SD | | 5.79 ± 0.70 | 6.18 ± 0.69 | 1.93 ± 0.46 |
| Intermittent WBV | 36 | 4.93 ± 0.13 | 4.67 ± 0.42 | 1.27 ± 0.07 |
| | 37 | 4.67 ± 0.21 | 5.38 ± 0.00 | 1.20 ± 0.08 |
| | 38 | 4.74 ± 0.11 | 5.54 ± 0.18 | 1.24 ± 0.03 |
| | 39 | 4.67 ± 0.13 | 5.55 ± 0.68 | 1.24 ± 0.01 |
| | 40 | 5.30 ± 1.06 | 6.53 ± 1.14 | 1.45 ± 0.36 |
| | 41 | 6.07 ± 0.10 | 7.35 ± 0.73 | 1.72 ± 0.03 |
| | 42 | 6.08 ± 0.10 | 6.87 ± 0.42 | 1.75 ± 0.06 |
| | 43 | 6.13 ± 0.02 | 7.40 ± 0.00 | 1.72 ± 0.02 |
| Intermittent WBV, mean ± SD | | 5.32 ± 0.67 | 6.16 ± 1.01 | 1.45 ± 0.25 |
| WBV, mean ± SD | | 5.52 ± 0.70 | 6.17 ± 0.86 | 1.66 ± 0.44 |

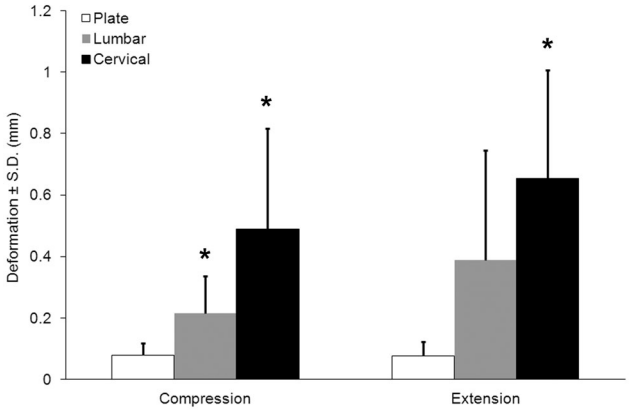


**Figure 3.** Compression and extension deformations in the cervical and lumbar regions during vibration exposure. The extent of compression in both the cervical and lumbar regions is significantly different than zero, while extension is only significant in the cervical region, as indicated by the asterisk (*). Also shown is the amount of deformation that was detected for the rigid plate during vibration, representing the small error associated with this method.

Deformations were induced in both the cervical and lumbar regions during vibration (Fig. 3). Both compression ($0.215 \pm 0.122$ mm) and extension ($0.388 \pm 0.356$ mm) were induced in the lumbar spine (Fig. 3), with the extent of compression being significant ($p = 0.019$), although extension was not significantly increased ($p = 0.064$). However, in the cervical region, the extent of both compression ($0.490 \pm 0.327$ mm; $p = 0.032$) and extension ($0.653 \pm 0.352$ mm; $p = 0.011$) was significant (Fig. 3).

Behavioral sensitivity was induced as early as Day 1 in both the hind paw and forepaw, regardless of the WBV exposure paradigm (Fig. 4). Specifically, the response threshold was significantly reduced in the hind paw at Day 1 after a single WBV exposure in both the *repeated WBV* ($p = 0.001$) and *intermittent WBV* ($p < 0.001$) groups (Fig. 4). However, only the *repeated WBV* exposure induced a decrease in threshold in the hind paw that was significantly lower ($p = 0.039$) than *sham* at all days (Fig. 4). In contrast, the response threshold remained at baseline levels at all time points following the *sham* exposure. The first vibration exposure in the *intermittent WBV* exposure paradigm induced only a transient decrease in withdrawal threshold in the hind paw that was significantly lower ($p = 0.004$) than baseline and was sustained through Day 5 (Fig. 4). Interestingly, when exposed to a second vibration (at Day 7), the resulting decrease in withdrawal threshold that was induced was sustained until Day 14 ($p = 0.039$), but did not decrease beyond withdrawal thresholds induced by the first exposure (Fig. 4).

Overall, both *repeated WBV* ($p < 0.0001$) and *intermittent WBV* ($p = 0.043$) induced significantly increased behavioral sensitivity in the forepaw compared to *sham* (Fig. 4). In fact, the behavioral sensitivity induced by *repeated WBV* was significantly lower ($p = 0.026$) than *intermittent WBV* (Fig. 4). The

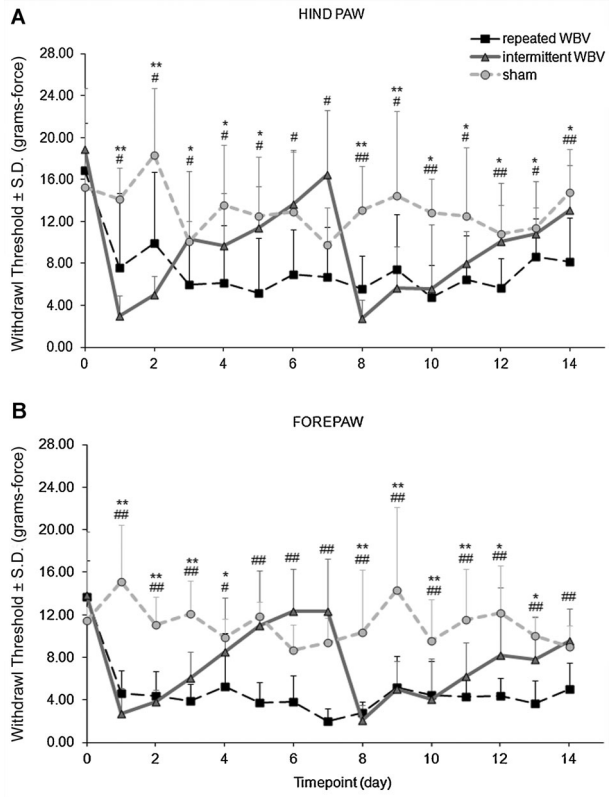


**Figure 4.** Withdrawal thresholds for *repeated WBV*, *intermittent WBV*, and *sham* groups in the forepaw and hind paw. A: The withdrawal threshold for the hind paw in the *repeated WBV* is significantly lower ($^{\#\#}p < 0.05$) than *sham* and baseline only on isolated days (Days 8, 10, 12, and 14), and is significantly lower ($^{\#}p < 0.04$) than only baseline on all other. *Intermittent WBV* is significantly lower ($^{**}p < 0.03$) than sham and baseline only on Days 1–2 and 8–9 and significantly lower ($^{*}p < 0.05$) than only baseline on Days 3–5 and 10–14. B: The threshold for forepaw withdrawal is significantly lower ($^{\#\#}p < 0.05$) in the *repeated WBV* group compared to *sham* and baseline on all days, except Day 4, but is significantly lower ($^{\#}p < 0.03$) than baseline on Day 4. *Intermittent WBV* is significantly ($^{**}p < 0.05$) different from *sham* and baseline on Days 1–3 and 8–11, and significantly different ($^{*}p < 0.05$) from baseline on Days 4, 12, and 13.

threshold for forepaw withdrawal was significantly lower ($p < 0.05$) in the *repeated WBV* group compared to *sham* on all days except Day 4, whereas *intermittent WBV* exposure was only different from *sham* on Days 1–3 and Days 8–11 (Fig. 4). Similar to the hind paw responses, *repeated WBV* exposure reduced ($p < 0.03$) the forepaw withdrawal threshold below baseline levels throughout the entire testing period regardless of whether during the loading or rest period (Fig. 4). *Intermittent WBV* exposure induced a reduction in withdrawal threshold in the forepaw that was transient, but for a shorter period than was observed in the hind paw, lasting only 4 days after the first exposure and 6 days after the second exposure (Fig. 4). The rate of recovery in the forepaw was significantly slower ($p = 0.036$) after the second vibration exposure ($1.15 \pm 0.39$ g/day) than after the first exposure ($1.82 \pm .707$ g/day) (Fig. 4). In contrast, the rate of recovery was not different between the first and second exposure in the hind paw (Fig. 4).

## DISCUSSION

This study demonstrates that even a single exposure of whole body vibration is sufficient to induce immediate and transient behavioral sensitivity in both the forepaw and hind paw, and that repeated exposure produces a sustained response (Fig. 4), substantiating WBV as a potential mechanism of producing pain. Although our in vivo pain model of whole body vibration in the rat appears to induce pain, there were no other adverse effects of the vibration, with all rats exhibiting normal weight gain consistent with that of naïve rats over a typical 14 day period. Neither the acceleration of the vibrating plate ($5.52 \pm 0.70$ m/s$^2$; $0.56 \pm 0.07$ g) nor of the rat ($6.17 \pm 1.01$ m/s$^2$; $0.63 \pm 0.09$ g) were different between groups in our study. Of note, control of the rat acceleration was the primary goal in establishing this new model. Nonetheless, both of these values fall in the range of the acceleration magnitudes used in other transmissibility studies using both humans and other species, which range from 0.1 to 5 g[7–10]; the 15 Hz vibration frequency is also within the range of frequencies (4.5–60 Hz) reported in other animal studies.[8,10] Although the behavioral results of our study reflect outcomes only for a single vibration amplitude and frequency, that vibration profile is sufficient to produce behavioral sensitivity. In addition, the accelerometer was not mounted to the spine and so measurements do not reflect those of the spinal response alone. However, pilot studies (unpublished) indicate these responses to be similar for 15 Hz, especially under conditions with passive muscle contributions. Additional studies at different frequencies and amplitudes will help characterize injury resulting from WBV.

The sustained sensitivity that is produced in both the forepaw and hind paw by the *repeated WBV* exposure (Fig. 4) suggests that such exposure for even seven days is sufficient to induce chronic injury or a sustained modification in the nociceptive cascades. In contrast, although a single exposure induces behavioral sensitivity, it is short-lived and lasts only for 4 or 5 days in the forepaw and hind paw, respectively (Fig. 4). Interestingly, even though this resolves by Day 6 in the *intermittent WBV* group and returns to baseline levels, it is immediately re-established after the second exposure, but takes longer to resolve and exhibits a slower rate of recovery after a second exposure (Fig. 4). This heightened, longer-lasting behavioral sensitivity after a rest period and re-exposure suggests that the initial exposure may reduce the pain threshold or modulate the central mechanisms that contribute to pain so that the subsequent second exposure produces a more "severe" response than does the same exposure initially. This longer-duration of sensitivity after a re-exposure is consistent with the behavioral sensitivity response in a study in which the L5 lumbar nerve root was ligated and re-injured again 6 weeks later.[15] In that study, the behavioral response after the second injury was significantly increased over the response after the first injury.[15] However, no such similar increase in behavioral sensitivity was observed in the current study (Fig. 4), which may be due to the fact that a WBV induces a less-robust tissue injury. However, it is also possible that since the initial WBV reduces the response threshold to approximately 4 g-force (Fig. 4), this testing technique may not enable detection of an additional decrease in response threshold since there are only three other filaments (0.6, 1.4, and 2.0 g-force), with lower strengths, providing limited resolution to detect any changes between the first and second exposures. Nonetheless, additional studies using other measures of behavioral assessment may help characterize the extent and type of pain and functional deficits that may result from WBV.

The production of behavioral sensitivity after WBV is consistent with other models of pain from mechanical tissue loading.[13,15–17] A single transient mechanical loading to isolated nerve roots and facet joints in the cervical spine induces an immediate and sustained decrease in the response threshold.[13,17] Similarly, separate injuries to the lumbar nerve root or sciatic nerve also induce a sustained increase in behavioral sensitivity.[15,16] The behavioral data from those studies help to contextualize the extent and severity of tissue injury throughout the spine that may be responsible for pain after a WBV exposure. The *repeated WBV* induces sensitivity in both paws up to Day 14 (Fig. 4), but the behavioral assessments were performed for only 14 days, so long-term outcomes in these models still remain undetermined.

Although vibration exposure was imposed to the whole body (Fig. 2), there were differences detected between the withdrawal threshold of the forepaw and hind paw and between the deformation responses of the cervical and lumbar regions (Figs. 3 and 4). Both paws exhibited an overall difference in response threshold compared to *sham* for the *repeated WBV* group, but only the forepaw response was different from *sham* for the *intermittent WBV* group (Fig. 4). Also, the threshold for forepaw withdrawal was significantly lower in the *repeated WBV* group compared to *sham* on all days except Day 4, whereas it was only different on Days 8, 10, 12, and 14 compared to *sham* in the hind paw (Fig. 4). These differences in behavioral sensitivity may be due to the differences in compression and extension in the cervical and lumbar region during vibration. It is possible that the reduced paw withdrawal thresholds may be due to local effects of their direct loading. Yet, this is unlikely since such mechanical contributions were small; additional studies assaying tissues for markers of local injury will provide additional insight about whether WBV induces local, central, or combined effects leading to pain. Both compression and extension were induced in the lumbar and cervical spines (Fig. 3), with the extent of compression being significant in both, while extension was only increased in the cervical region. The extent of compression in the cervical region was nearly

double that in the lumbar region and cervical extension was 1.5 times greater than lumbar extension, which may be responsible for the more robust sensitivity in forepaw (Figs. 3 and 4).

This study suggests that a repeated WBV exposure for 30 min of 15 Hz vibration at a magnitude of 0.56 g establishes pain. Although vibration exposure was performed under inhalation anesthesia, which eliminates any contribution of the active musculature, this was still sufficient to induce behavioral sensitivity. Additional studies are needed to further define the role of active musculature in this and other similar models. Indeed, previous animal studies, also using anesthesia, have linked WBV to pain over a range of frequencies from 4.5 to 60 Hz.[8,10] Several neuropeptides related to nociception have been reported to change in the rabbit after a single 2 hr WBV exposure at 4.5 Hz with an amplitude of.0.35 g.[8] Substance P in the L4–L6 dorsal root ganglia decreased and vasoactive intestinal peptide increased as early as 30 min after a single WBV exposure, which is consistent with results seen in other painful peripheral nerve injuries.[8,18] In addition, arterial endothelial cell disruption has been reported to occur as early as 45 min after vibration of the tail at 60 Hz for 4 h in a rat.[10] Together, the molecular and cellular changes related to nociception and injury that have been reported in these other animal studies support the link between WBV exposure and pain, even for varying frequencies and amplitudes of exposures. Although the current study did not explicitly investigate the relationship between behavioral sensitivity and relevant physiological cascades related to pain, the results do demonstrate increased behavioral sensitivity after two different WBV exposure paradigms and suggest such future investigations to be worthwhile.

This model of vibration injury serves as a tool to further investigate the relationship between WBV and pain. Although the current study supports the hypothesis that vibration leads to pain, it does not identify the source of such modifications. Continued studies under different vibration conditions and incorporating assays of tissue mechanics, as well as markers of injury, inflammation and nociception, will enable a more complete definition of the relationship(s) between pain and injury. In particular, studies assaying neuroinflammatory responses in muscle, disc, and other tissues, together with expanded behavioral assessments will provide added insight about this type of painful injury.

## ACKNOWLEDGMENTS

Thanks to Dr. Nicolas Jaumard for input on device fabrication and mechanical analyses.

## REFERENCES

1. Boshuizen HC, Bongers PM, Hulshof CT. 1992. Self-reported back pain in fork-lift truck and freight-container tractor drivers exposed to whole-body vibration. Spine 17:59–65.
2. Bovenzi M, Hulshof CTJ. 1988. An updated review of epidemiologic studies on the relationship between exposure to whole-body vibration and low back pain (1986–1997). Int Arch Occup Environ Health 72:351–365.
3. Boshuizen HC, Bongers PM, Hulshof CT. 1999. Effect of whole body vibration on low back pain. Spine 24:2506–2515.
4. Nevin RL, Means GE. 2009. Pain and discomfort in deployed helicopter aviators wearing body armor. Aviat Space Environ Med 80:807–810.
5. Kelsey JL, Hardy RJ. 1975. Driving of motor vehicles as a risk factor for acute herniated lumbar intervertebral disc. Am J Epidemiol 102:63–73.
6. Panjabi MM, Andersson GJ, Jorenus L. 1986. In vivo measurements of spinal column vibrations. J Bone Joint Surg 68:695–702.
7. Mansfield NJ, Griffin MJ. 2000. Non-linearities in apparent mass and transmissibility during exposure to whole-body vertical vibration. J Biomech 33:933–941.
8. Weinstein J, Pope M, Schmidt R, et al. 1988. Neuropharmacologic effects of vibration on the dorsal root ganglion. Spine 13:521–525.
9. Smith SD, Kazarian LE. 1994. The effects of acceleration on the mechanical impedance response of a primate model exposed to sinusoidal vibration. Ann Biomed Eng 22:78–87.
10. Curry BD, Bain JLW, Riley DA. 2002. Vibration injury damages arterial endothelial cells. Muscle Nerve 25:527–534.
11. Zimmerman M. 1983. Ethical guidelines for investigations of experimental pain in conscious animals. Pain 16:109–110.
12. Chaplan SR, Bach FW, Pogrel JW, et al. 1994. Quantitative assessment of tactile allodynia in the rat paw. J Neurosci Meth 53:55–63.
13. Lee KE, Davis MB, Winkelstein BA. 2008. Capsular ligament involvement in the development of mechanical hyperalgesia after facet joint loading: behavioral and inflammatory outcomes in a rodent model of pain. J Neurotrauma 25:1383–1393.
14. Dong L, Guarino BB, Jordan-Sciutto KL, et al. 2011. Activating transcription factor 4, a mediator of the integrated stress response, is increased in the dorsal root ganglia following painful facet joint distraction. Neuroscience 193: 377–386.
15. Hunt JL, Winkelstein BA, Rutowski MD, et al. 2001. Repeated injury to the lumbar nerve roots produces enhanced mechanical allodynia and persistent spinal neuroinflammation. Spine 26:2073–2079.
16. Willenbring S, DeLeo JA, Coombs DW. 1994. Differential behavioral outcomes in the sciatic cryoneurolysis model of neuropathic pain in rats. Pain 5:135–140.
17. Hubbard RD, Winkelstein BA. 2005. Transient cervical nerve root compression in the rat induces bilateral forepaw allodynia and spinal glial activation: mechanical factors in painful neck injuries. Spine 30:1924–1932.
18. Shehab SA, Atkinson ME. 1986. Vasoactive intestinal peptide increases in the spinal cord after peripheral axotomy of the sciatic nerve originate from primary afferent neurons. Brain Res 372:37–44.

**A3.** Acceleration data for 8 Hz vibration frequency.

| D0 | | | |
|---|---|---|---|
| **Rat** | **RMS Plate** | **RMS Rat** | **LVDT** |
| 109 | 3.985515 | 3.193409 | 4.74958 |
| 110 | 4.027893 | 3.143089 | 4.793946 |
| 111 | 3.907187 | 3.61468 | 4.655881 |
| 113 | 3.794509 | 4.150216 | 4.39923 |
| 114 | 3.744923 | 3.971156 | 4.341276 |
| 115 | 3.634413 | 4.493729 | 4.265104 |
| 116 | 3.695685 | 4.871007 | 4.290636 |
| Averages | 3.82716071 | 3.919612 | 4.499379 |
| SD | 0.14946597 | 0.647294 | 0.226329 |

| D7 | | | |
|---|---|---|---|
| **Rat** | **RMS Plate** | **RMS Rat** | **LVDT** |
| 109 | 3.813705 | 2.575236 | 4.4326 |
| 110 | 3.777131 | 2.812694 | 4.32285 |
| 111 | 3.769309 | 3.756788 | 4.387276 |
| 113 | 3.729225 | 4.414765 | 4.319654 |
| 114 | 3.766881 | 4.217479 | 4.342244 |
| 115 | 3.690905 | 4.284913 | 4.231665 |
| 116 | 3.613435 | 4.087653 | 4.1546 |
| Averages | 3.73722729 | 4.15232 | 4.312984 |
| SD | 0.06693784 | 0.743618 | 0.093562 |

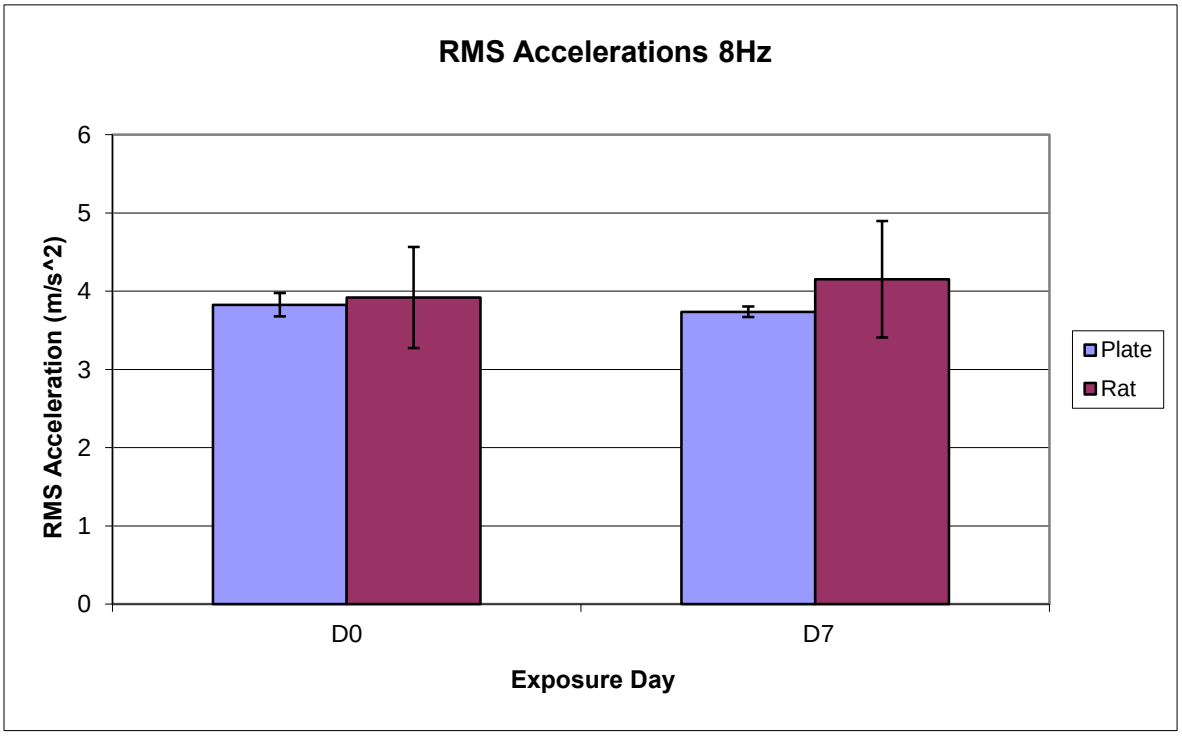

**A4.** Abstract presented at ASME Mtg. in June, 2013.

Proceedings of the ASME 2013 Summer Bioengineering Conference
SBC2013
June 26-29, Sunriver, Oregon, USA

**SBC2013-14111**

# A THREE DEGREE OF FREEDOM LUMPED PARAMETER MODEL OF WHOLE BODY VIBRATION ALONG THE SPINE IN THE RAT

**Nicolas V. Jaumard, Hassam A. Baig, Benjamin B. Guarino, Beth A. Winkelstein**

Spine Pain Research Lab
Department of Bioengineering
University of Pennsylvania
Philadelphia, PA 19104
USA

## INTRODUCTION

Whole body vibration (WBV) can induce a host of pathologies, including muscle fatigue and neck and low back pain [1,2]. A new model of WBV in the rat has been developed to define relationships between WBV exposures, kinematics, and behavioral sensitivity (i.e. pain) [3]. Although in vivo studies provide valuable associations between biomechanics and physiology, they are not able to fully define the mechanical loading of specific spinal regions and/or the tissues that may undergo injurious loading or deformation. Mathematical models of seated humans and primates have been used to estimate spinal loads and design measures that mitigate them during WBV [4-6]. Although such models provide estimates of relative spinal motions, they have limited utility for relating potentially pathological effects of vibration-induced kinematics and kinetics since those models do not enable simultaneous evaluation of relevant spinal tissues with the potential for injury and pain generation. As such, the goal of this work was to develop and validate a three degree of freedom (3DOF) lumped-parameter model of the prone rat undergoing WBV directed along the long-axis of the spine. The model was constructed with dimensions of a generalized rat and model parameters optimized using kinematics over a range of frequencies. It was validated by comparing predicted and measured transmissibility and further used to predict spinal extension and compression, as well as acceleration, during WBV for frequencies known to produce resonance in the seated human and pain in the rat [3,7].

## METHODS

The 3DOF lumped-parameter model of a rat fixed to a vibrating platform was constructed with 3 masses representing the head and shoulders (M1), trunk (M2), and pelvis and hind legs (M3) (Fig. 1). The masses were taken as 34%, 39% and 27% of the total rat body mass, respectively, based on measurements of the relative length of each corresponding body segment normalized to total body length. Springs and dampers connect the body segment masses to simulate the nonlinear mechanical behavior of the hard and soft tissues between the body segments (K1, K3; C1, C3) and between the body segments and the straps (K2, K4, K5; C2, C4, C5) used to secure the rat (Fig. 1). A custom Matlab script solved the differential equations describing the system in order to compute the mass displacements (x1(t), x2(t), x3(t)) as a function of the masses, spring coefficients, damper coefficients, input platform motion u(t).

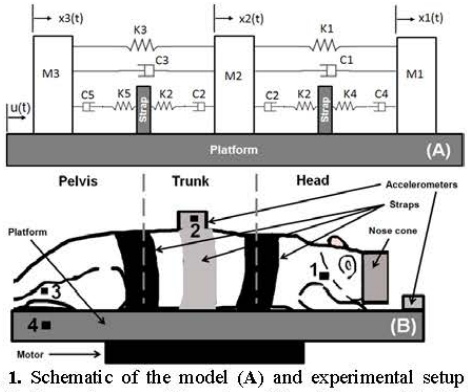


**Fig. 1.** Schematic of the model (**A**) and experimental setup (**B**), with the lumped masses (M), springs (K) and dampers (C). Markers are placed on the rat (1, 3), the trunk accelerometer (2), and the vibrating platform (4). Black straps secure the rat to the platform.

Biomechanical experiments using male Holtzman rats (n=14; 310-350g) affixed to the rigid platform via straps (Fig. 1B) were used to measure the displacements of the body segments during WBV in order to optimize and validate the model [3]. Rats underwent sinusoidal vibrations with a 1.5mm peak-to-peak amplitude, ranging from 3-15Hz, in discrete increments. A high-speed camera tracked markers on the rat's head, hind quarters (in leg/pelvis region), trunk, and the platform (Fig. 1B), at 120Hz during each input frequency. The displacements of the platform, head, trunk, and hind quarters were determined using the motion of the markers for each applied vibration.

A subset of rats (n=4) was used to optimize the parameters (K's, C's) in the model through comparing the transmissibility responses of the model and rats. Based on initial values of the parameters from pilot simulations and the average platform motion (u(t)) from the experiments, the theoretical displacements ($x_i(t)$) of the masses were computed. The root-mean square (RMS) of the displacements for the body segments and platform was calculated and used to compute the transmissibility of each body segment (head, trunk, pelvis) over the frequency ranges. Optimization of the model parameters was performed by comparing the experimental and predicted transmissibilities, as is customary [1,8]. The optimal K and C parameters were determined iteratively by minimizing the error between the trunk transmissibilities. The optimized model was then validated by comparing the predicted trunk transmissibility to the average trunk transmissibility at each frequency for a separate set of rats (n=4). The goodness-of-fit, $\varepsilon$, between the model and the experimental transmissibility profiles was calculated (eq. 1), where $\tau_i$ is the transmissibility at frequency $i$ and $N$ is the total number of frequencies [9] and compared using an F-test.

$$\varepsilon = 1 - \frac{\sqrt{\sum_3^{15}(\tau_{i,theo}-\tau_{i,exp})/(N-2)}}{(\sum_3^{15}\tau_{i,theo})/N} \quad \text{(eq.1)}$$

Data from an additional subset of rats (n=6) was used to compare the spinal motions and accelerations predicted by the optimized model for a 15Hz WBV. Cervical and lumbar motions were calculated from the model as the differences in displacements between the head (M1) and trunk (M2), x2(t)-x1(t), and between the trunk (M2) and pelvis (M3), x3(t)-x2(t) (Fig. 1). Also, the predicted trunk RMS acceleration was derived from the predicted trunk displacement and compared to the average RMS acceleration that was measured at the trunk using a uniaxial accelerometer strapped to the rat's thoracic spine (Fig. 1B).

## RESULTS

The spring and damper coefficients that yielded the best goodness-of-fit are: K1=750, K2=250, K3=750, K4=350, K5=500 N/m; C1=9.5, C2=9.5, C3=9.5, C4=9.5, C5=9.5 N.s/m. The best fit between the model and average experimental trunk transmissibility response was 88% (F=0.82; Fc=2.82) (Fig. 2). The optimized model had a goodness-of-fit of 90% (F=0.54; Fc=2.82) in predicting trunk transmissibility for the second set of rats (Fig. 2).

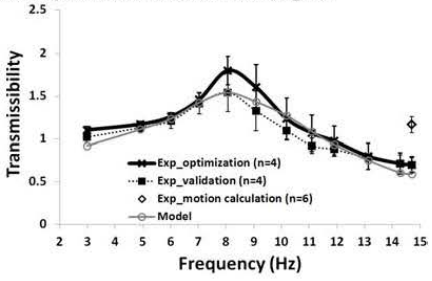


**Fig. 2.** Predicted & average experimental trunk transmissibility.

The predicted extensions and compressions of the cervical and lumbar spines were 3-5 fold less than the average values measured experimentally (Fig. 3A). Similarly, the model underestimated the trunk acceleration, with the predicted trunk RMS acceleration at 45% of the average experimental accelerations (Fig. 3B).

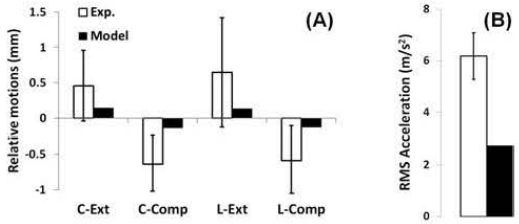


**Fig. 3.** Experimental and predicted extension (Ext) and compression (Comp) of the cervical (C) and lumbar (L) spines (**A**) and the trunk RMS acceleration (**B**) for 15HzWBV.

## DISCUSSION

Similar to other models of WBV [5,6], this model provides a reasonable estimation (90%) of thoracic transmissibility of the rat for WBV frequencies ranging from 3-15Hz (Fig.2). However, the predicted spinal motions and trunk acceleration were not as closely matched by the model (Fig. 3), and were consistently over-estimated by as much as 5 times. The model was only evaluated at a single frequency (15Hz) and predicted motions were consistently within 1.5 standard deviations of their corresponding average experimental values (Fig. 3). The model was developed and optimized over a range of frequencies (3-15Hz; Fig. 2), which may also contribute to its lack of performance at a given frequency at the extreme of that range. Of note, the group of rats used for the motion prediction aspect of this study was sedated and alive, while the other groups used expired rats, which may contribute to a difference in transmissibility during WBV. In fact, the transmissibility response of the group of rats used for the motion calculations also exhibited a much greater transmissibility (~1.16) than either of the other two sets of rats (0.70, 0.73) at 15Hz (Fig. 2). Continued optimization and validation of this model using data from sedated subjects will improve its utility. Nonetheless, the current findings provide a promising foundation for such future work.

Although more work is needed with parametric and sensitivity analyses, as well as more extensive validation studies, this 3DOF lumped-parameter model helps understand WBV. Even this simple model has utility to guide additional studies investigating the effects of WBV frequency and magnitude, and provides complementary biomechanical context for in vivo studies. It can help identify WBV exposures with the greatest injury risk and provide detailed insight about biodynamic responses of the spine and its tissues during WBV.


## ACKNOWLEDGMENTS

Support from the Department of Defense (W81XWH-10-2-0140).


## REFERENCES


1. Liang C, Chiang C (2006) *Int J Ind Ergonom* 36:869-90.
2. Mayton A, Kittusamy N, et al (2008) *Int J Ind Ergonom* 38:758-66.
3. Baig H, Guarino B, et al (2012) *J Orthop Res* submitted.
4. Smith S, Kazarian L (1994) *Ann Biomed Eng* 22:78-87.
5. Fritton J, Rubin C, et al (1997) *Ann Biomed Eng* 25:831-9.
6. Wang W, Bazrgari B, et al (2010) *Ind Health* 48:557-64.
7. Kitazaki S, Griffin M (1997) *J Sound Vib* 200:83-103.
8. Kiiski J, Heinonen A, et al (2008) *J Bone Miner Res* 23:1318-25.
9. Wong J (1989) Terramechanics and Off-Road Vehicles. Elsevier.

**A5.** Optimum values for the mass, springs, and dampers of the lumped-parameter model of a rat subjected to WBV

| **Mass (% total mass $M_T$)** | | **Stiffness coefficients (N/m)** | | **Damping coefficients (N.s/m)** | |
|---|---|---|---|---|---|
| **M1** | 26±2.4 | **K1** | 600 | **C1** | 3 |
| **M2** | 37±4.3 | **K2** | 200 | **C2** | 50 |
| **M3** | 36±2.9 | **K3** | 700 | **C3** | 12 |
| | | **K4** | 450 | **C4** | 11 |
| | | **K5** | 675 | **C5** | 11.5 |

**A6.** Detailed inventory of tissues harvested to date.

| ## | surgeon | injury | Study name/date | Timepoin | type harv | cervical spinal enla | lumbar spinal enla | brain | C-Disc | L-Disc | upper mm | lower mm | gastroc | Skin | Shelf 2; f |
|---|---|---|---|---|---|---|---|---|---|---|---|---|---|---|---|
| 1 | bbg/hab | 15 Hz Repeated | 05-2011 vibration pilot stu | d14 | fresh | a, d: homog | used (homog) | | homg. (western) | | ex + fresh | | | not taken | |
| 2 | bbg/hab | 15 Hz Repeated | | d14 | fresh | a,c: homg. b: tissue | used (homog) | | homg. (western) | | | | | | |
| 3 | bbg/hab | 15 Hz Repeated | | d14 | fresh | a,c: homg. b: tissue | used (homog) | | ? | | | | | | |
| 4 | bbg/hab | 15 Hz Repeated | | d14 | fresh | a,b: homg | used (homog) | | homg. (western) | homg. (western) | | | | | |
| 6 | bbg/hab | 5 Hz Repeated | | d14 | fresh | a: homg. b&c: tissub: homg. a&c: tiss | | | homg. (western) | homg. (western) | | | | | |
| 7 | bbg/hab | 5 Hz Repeated | | d14 | fresh | a: homg. b&c: tissub: homg. a&c: tiss | | | homg. (western) | homg. (western) | | | | | no spinal |
| 8 | bbg/hab | 5 Hz Repeated | | d14 | fresh | a: homg. b&c: tissub: homg. a&c: tiss | | | homg. (western) | | | | | | no spinal |
| 9 | bbg/hab | normal | | - | fresh | a homg b&c tissue a&c homg ; b tissu | | | homg. (western) | homg. (western) | x | x | x | | no spinal |
| 10 | bbg/hab | normal | | - | fresh | a homg b&c tissue a&c homg ; b tissu | | | homg. (western) | | x | x | | | no spinal |
| 11 | bbg/hab | normal | | - | fresh | a homg b&c tissue a&c homg ; b tissu | | | homg. (western) | homg. (western) | ex + fresh | | | | no spinal |
| 12 | bbg/hab | 15 Hz Repeated | 10-2011 vibration round 2 | d14 | fresh | a: homg | used (homog?) | | homg. (western) | | | | | | no spinal |
| 13 | bbg/hab | 15 Hz Repeated | | d14 | fresh | a: homg, b: tissue | used (homog?) | | homg. (western) | | embedded | | | | no spinal |
| 15 | bbg/hab | 15 Hz Repeated | | d14 | fresh | a: homg | used (homog?) | | ? | | | | | | no spinal |
| 16 | bbg/hab | anesthesia sham | | d14 | fresh | a: homg | used (homog?) | | homg. (western) | | 2xtubes; ex | | | | no spinal |
| 17 | bbg/hab | anesthesia sham | | d14 | fresh | a: homg | used (homog?) | | homg. (western) | | x | | | | no spinal |
| 18 | bbg/hab | anesthesia sham | | d14 | fresh | a: homg | used (homog?) | | homg. (western) | | | | | | no spinal |
| 19 | bbg/hab | anesthesia sham | | d14 | fresh | a: homg | used (homog?) | | homg. (western) | | | | | | no spinal |
| 20 | bbg/hab | 15 Hz Repeated | 01-2012 vibration round 3 | d14 | fixed | sectioned | sectioned | 30% sucrose | Sectioned 4/13-16 (gel) | 10% EDTA on 4-13-2 | cut5 | embedded | embedded | | |
| 21 | bbg/hab | 15 Hz Repeated | | d14 | fixed | embedded | embedded | 30% sucrose | Sectioned 4/13-16 (gel) | 10% EDTA on 4-13-2 | cut5 | embedded | embedded | | |
| 23 | bbg/hab | 15 Hz Repeated | | d14 | fixed | sectioned | sectioned | 30% sucrose | Sectioned 4/13-16 (gel) | sectioned | embedded | embedded | embedded | | |
| 24 | bbg/hab | 15 Hz Repeated | | d14 | fixed | embedded | sectioned | 30% sucrose | Sectioned 4/13-16 (gel) | 10% EDTA on 4-13-2 | embedded | embedded | embedded | | |
| 26 | bbg/hab | 15 Hz Repeated | | d14 | fresh | b,d: homg | used (homog) | | homg. (western); RNA; ti | | | | | | |
| 27 | bbg/hab | 15 Hz Repeated | | d14 | fresh | c,d: homg. a&b: tissued | (homog) | | homg. (western); RNA; ti | | | | | | |
| 28 | bbg/hab | anesthesia sham | | d14 | fresh | c,d: homg. a&b: tissued | (homog) | | homg. (western); RNA; ti | remain in 10% EDTA | cut5 | embedded | embedded | | |
| 29 | bbg/hab | anesthesia sham | | d14 | fresh | c,d: homg. a&b: tissued | (homog) | | homg. (western); RNA; ti | remain in 10% EDTA | embedded | embedded | embedded | | |
| 30 | bbg/hab | anesthesia sham | | d14 | fresh | c,d: homg. a&b: tissued | (homog) | | homg. (western); RNA; ti | remain in 10% EDTA | embedded | embedded | embedded | | |
| 31 | bbg/hab | anesthesia sham | | d14 | fresh | c,d: homg. a&b: tissued | (homog) | | homg. (western); RNA; ti | | | | | | |
| 32 | bbg/hab | anesthesia sham | 02-2012 round 4 (sham or | d14 | fixed | sectioned | sectioned | 30% sucrose | sectioned | remain in 10% EDTA | cut5 | embedded | embedded | | |
| 33 | bbg/hab | anesthesia sham | | d14 | fixed | embedded | embedded | 30% sucrose | sectioned | remain in 10% EDTA | cut5 | embedded | embedded | | |
| 34 | bbg/hab | anesthesia sham | | d14 | fixed | embedded | embedded | 30% sucrose | sectioned | remain in 10% EDTA | embedded | embedded | embedded | | |
| 35 | bbg/hab | anesthesia sham | | d14 | fixed | embedded | embedded | 30% sucrose | 10% EDTA | remain in 10% EDTA | embedded | embedded | embedded | | |
| 36 | bbg/hab | Intermittent 15 Hz | 04-2012 round 5 1 day 1 | d14 | fixed (c. sp c | tissue | tissue | | sectioned (no gelatin) | 10% EDTA | | | | | |
| 37 | bbg/hab | Intermittent 15 Hz | | d14 | fixed (c. sp c | tissue | tissue | | sectioned (no gelatin) | 10% EDTA | cut5 | | | | |
| 38 | bbg/hab | Intermittent 15 Hz | | d14 | fixed (c. sp c | tissue | tissue | | sectioned (no gelatin) | 10% EDTA | cut5 | | | | |
| 39 | bbg/hab | Intermittent 15 Hz | | d14 | fixed (c. sp c | tissue | tissue | | | 10% EDTA | | | | | |
| 40 | bbg/hab | Intermittent 15 Hz | | D14 | fresh | tissue | tissue | | Left out of -80? | Left out of -80? | ex + fresh | | | | |
| 41 | bbg/hab | Intermittent 15 Hz | | D14 | fresh | tissue | tissue | | Left out of -80? | Left out of -80? | | | | | |
| 42 | bbg/hab | Intermittent 15 Hz | | D14 | fresh | tissue | tissue | | Left out of -80? | Left out of -80? | | | | | |
| 43 | bbg/hab | Intermittent 15 Hz | | D14 | fresh | tissue | tissue | | Left out of -80? | Left out of -80? | | | | | |
| 44 | JLB/HAB | time course D1 (D1R) | Vibration time course D1 l | d1 | fresh | | | | | | ex + fresh | | | | |
| 45 | JLB/HAB | time course D1 | | d1 | fresh | | | | | | | | | | |
| 46 | JLB/HAB | time course D1 | | d1 | fresh | | | | | | | | | | |
| 47 | JLB/HAB | time course D1 | | d1 | fresh | | | | | | | | | | |
| 48 | JLB/HAB | time course D1 | | d1 | fresh | | | | | | | | | | |
| 49 | JLB/HAB | time course D1 | | d1 | fresh | | | | | | | | | | |
| 50 | JLB/HAB | time course D1 | | d1 | fresh | | | | | | | | | | |
| 51 | JLB/HAB | time course D1 | | d1 | fresh | | | | | | | | | | |
| 52 | hab/sk | Repeated 15 Hz | 08-07-12 Repeated Vibrat | d7 | fresh | | | | | | | | | | |
| 54 | hab/sk | Repeated 15 Hz | | d7 | fresh | | | | | | | | | | |
| 56 | hab/sk | Repeated 15 Hz | | d7 | fresh | | | | | | | | | | |
| 57 | hab/sk | Repeated 15 Hz | | d7 | fresh | | not taken....retract | | 10% EDTA | | | | | | |
| 59 | hab/sk | Repeated 15 Hz | died at day 1 immersed in | D1 | fixed | | | | 10% EDTA | 10% EDTA | | | | | |
| 60 | D/C | | | ----- | | | | | | | | | | | |
| 61 | D/C | | | ----- | | | | | | | | | | | |
| 62 | hab/sk | intermittent 15 Hz only D1 | | D7 | fresh | | | | | | ex + fresh | | | | |
| 63 | hab/sk | intermittent 15 Hz only D1 | tubes labeled 64 | D7 | fresh | | | | | | | | | | |
| 64 | hab/sk | intermittent 15 Hz only D1 | tubes labeled 63 | D7 | fresh | | | | | | | | | | |
| 65 | hab/sk | intermittent 15 Hz D1 and | | D8 | fresh | | | | | | ex + fresh | | | | |
| 66 | hab/sk | intermittent 15 Hz D1 and | | D8 | fresh | | | | | | | | | | |
| 67 | hab/sk | intermittent 15 Hz D1 and | | D8 | fresh | | | | | | | | | | |
| 68 | hab/sk | Sham | 8-22-12 Anesthesia Contr | D1 | fresh | | | | | | ex + fresh | | | | |
| 69 | hab/sk | Sham | | D1 | fresh | | | | | | | | | | |
| 70 | hab/sk | Sham | | D1 | fresh | | | | | | | | | | |
| 71 | hab/sk | Sham | check beh | D1 | fresh | | | | | | | | | | |
| 72 | hab/sk | 15 Hz Day 1 | 8-30-12 Fixed D1 Vibratio | D1 | fixed | 30% sucrose | 30% sucrose | | 10% EDTA | 10% EDTA | 30% sucrose | 30% sucrose | 30% sucros | | Cold Roo |
| 73 | hab/sk | 15 Hz Day 1 | | D1 | fixed | 30% sucrose | 30% sucrose | 30% sucrose | 10% EDTA | 10% EDTA | 30% sucrose | 30% sucrose | 30% sucros | | Cold Roo |
| 74 | hab/sk | 15 Hz Day 1 | | D1 | fixed | 30% sucrose | 30% sucrose | 30% sucrose | 10% EDTA | 10% EDTA | 30% sucrose | 30% sucrose | 30% sucros | | Cold Roo |
| 75 | hab/sk | 15 Hz Day 1 | | D1 | fixed | 30% sucrose | 30% sucrose | 30% sucrose | 10% EDTA | 10% EDTA | 30% sucrose | 30% sucrose | 30% sucros | | Cold Roo |

| ## | surgeon( | injury | Study name/date | Timepoin | type harv | cervical spinal enla | lumber spinal enla | brain | C-Disc | L-Disc | upper mm | lower mm | gastroc | Skin | Shelf 2; F |
|---|---|---|---|---|---|---|---|---|---|---|---|---|---|---|---|
| 76 | hab/sk | Repeated | | D8 | fresh | | | | | | ex + fresh | | | | |
| 77 | hab/sk | Repeated | | D8 | fresh | | | | | | | | | | |
| 78 | hab/sk | Repeated | | D8 | fresh | | | | | | | | | | |
| 79 | hab/sk | Repeated | | D8 | fresh | | | | | | | | | | |
| 80 | hab/sk | Sham | | D7 | fresh | | | | | | ex + fresh | | | | |
| 81 | hab/sk | Sham | | D7 | fresh | | | | | | | | | | |
| 82 | hab/sk | Sham | | D7 | fresh | | | | | | | | | | |
| 83 | hab/sk | Sham | | D7 | fresh | | | | | | | | | | |
| 84 | hab/sk | Sham | | D8 | fresh | | | | | | ex + fresh | | | | |
| 85 | hab/sk | Intermittent | | D8 | fresh | | | | | | | | | | |
| 86 | hab/sk | Sham | | D8 | fresh | | | | | | | | | | |
| 87 | hab/sk | Intermittent | | D8 | fresh | | | | | | | | | | |
| 88 | hab/sk | Intermittent | | D8 | fresh | | | | | | | | | | |
| 89 | x | | | | | | | | | | | | | | |
| 90 | hab/sk | Sham | | D8 | fresh | | | | | | | | | | |
| 91 | hab/sk | Sham | | D8 | fresh | | | | | | | | | | |
| 92 | HSM | Repeated 15 Hz | 2/19/2013 | D14 | fresh | ex + fresh | | | ex + fresh | | | | | | also have |
| 93 | HSM | Repeated 15 Hz | | D14 | fresh | ex + fresh | | | ex + fresh | | | | | | " |
| 94 | HSM | Sham - Anesthesia | harvested 2/21/13 | D1 | fresh | | | | | | ex + fresh | | | | -80 |
| 95 | HSM | Sham - Anesthesia | | D1 | fresh | | | | | | ex + fresh | | | | |
| 96 | HSM | Sham - Anesthesia | harvested 2/22/13 | D1 | fixed | | | | | | embedded+ | | | | cold roon |
| 97 | HSM | Sham - Anesthesia | | D1 | fixed | | | | | | embedded+ | | | | |
| 98 | HSM | Sham - Anesthesia | | D1 | fixed | | | | | | embedded+ | | | | |
| 99 | HSM | Sham - Anesthesia | | D1 | fixed | | | | | | embedded+ | | | | |
| 100 | HSM | Repeated 15 Hz | harvested 5/2/13 | D14 | fresh | ex + fresh | | | ex + fresh | | | | | | have fres |
| 101 | HSM | Repeated 15 Hz | | D14 | fresh | ex + fresh | | | ex + fresh | | | | | | |
| 102 | HSM | Repeated 15 Hz | | D14 | fresh | ex + fresh | | | ex + fresh | | | | | | |
| 103 | HSM | Repeated 15 Hz | harvested 4/18/13 - died f | acute | fresh & fixed | fixed | xx | fixed | fixed | xx | fresh and fix | xx | fresh and fi | | this guy |
| 104 | HSM | Repeated 15 Hz | harvested 5/3/13 | D14 | fresh | ex + fresh | | | ex + fresh | | | | | | |
| 105 | HSM | Sham - Anesthesia | | D14 | fresh | ex + fresh | | | ex + fresh | | | | | | |
| 106 | HSM | Sham - Anesthesia | | D14 | fresh | ex + fresh | | | ex + fresh | | | | | | |
| 107 | HSM | Sham - Anesthesia | | D14 | fresh | ex + fresh | | | ex + fresh | | | | | | |
| 108 | HSM | Acute 8Hz | harvested 3 hrs after vibr | D0 | fresh | | | fixed | | didn't take | | | | | In N6/N7 |
| 109 | HSM | Intermittent 8Hz | pilot | D14 | | fresh | fresh | fixed | fixed | fixed | fresh and fix | fresh and fix | fresh and fi | fixed | in -80 |
| 110 | HSM | Intermittent 8Hz | | D14 | | fresh | fresh | fixed | fixed | fixed | fresh and fix | fresh and fix | fresh and fi | fixed | |
| 111 | HSM | Intermittent 8Hz | | D14 | | fresh | fresh | fixed | fixed | fixed | fresh and fix | fresh and fix | fresh and fi | fixed | |
| 112 | HSM | Acute 8Hz | died during 1st day of vib | D0 | harvested to | | | | | | | | | | |
| 113 | HSM | Intermittent 8Hz | | D14 | | fresh | fresh | fixed | fixed | fixed | fresh and fix | fresh and fix | fresh and fi | fixed | |
| 114 | HSM | Intermittent 8Hz | | D14 | | fresh | fresh | fixed | fixed | fixed | fresh and fix | fresh and fix | fresh and fi | fixed | |
| 115 | HSM | Intermittent 8Hz | | D14 | | fresh | fresh | fixed | fixed | fixed | fresh and fix | fresh and fix | fresh and fi | fixed | |
| 116 | HSM | Intermittent 8Hz | | D14 | | fresh | fresh | fixed | fixed | fixed | fresh and fix | fresh and fix | fresh and fi | fixed | |
| 117 | HSM | Intermittent 8Hz | displacement controls | D14 | | | | | | | | | | | |
| 118 | HSM | Intermittent 8Hz | | D14 | | | | | | | | | | | |
| 119 | HSM | Intermittent 8Hz | | D14 | | | | | | | | | | | |
| 120 | HSM | Intermittent 8Hz | | D14 | | | | | | | | | | | |
| 121 | HSM | Intermittent Sham | | D14 | | | | | | | | | | | |
| 122 | HSM | Intermittent Sham | | D14 | | | | | | | | | | | |
| 123 | HSM | Intermittent Sham | | D14 | | | | | | | | | | | |
| 124 | HSM | Intermittent Sham | | D14 | | | | | | | | | | | |

**A7.** Abstract Presented at AAE Mtg. in March, 2013.

Painful Whole-Body Vibration is Associated with Decreased BiP Expression in the Lumbar Spinal Cord

K Tanaka (1), HA Baig (2), BB Guarino(2), JR Smith (2), BA Winkelstein(2), KL Jordan-Sciutto (3)
(1)Department of Endodontics, School of Dental Medicine
(2)Department of Bioengineering, School of Engineering & Applied Science
(3)Department of Pathology, School of Dental Medicine
University of Pennsylvania

**Objective**: Chronic musculoskeletal orofacial pain can be misdiagnosed as a periapical pain in a clinical situation. Hyperalgesia, increased pain in response to a painful stimulus has been reported in patients experiencing chronic musculoskeletal orofacial pain. Whole-body vibration (WBV) has been linked to the development of chronic pain. Yet, the mechanism of its developmental and the cellular cascades responsible for its maintenance remain poorly defined. Specifically, while inflammation and cellular activation are known to be involved in pain, the role of mediators of the integrated stress response in spinal cells following painful exposures has not been investigated. The purpose of this study was to evaluate if a major chaperone protein of the endoplasmic reticulum (BiP) is modulated in the spinal cord in association with pain after WBV using a novel model in the rat.
**Methods**: All procedures were IACUC-approved. Holtzman rats (n=7) were exposed to a WBV at 15Hz for 30 minutes daily for 7 days. An additional group of rats (n=6) were exposed to anesthesia for that same period of 7 days to serve as the sham control group. All rats were assessed for behavioral sensitivity by measuring mechanical hyperalgesia during the exposure period and for another 7 days after that. Lumbar spinal cord was harvested 7 days after the cessation of the exposure to quantify BiP using western blot analysis. BiP expression for each sample was normalized by $\beta$-tublin levels and compared between WBV and sham using t-tests.
**Results**: WBV induced immediate behavioral sensitivity on day 1 that was sustained for 7 days after the cessation of the WBV exposure ($p=0.01$).BiP expression levels in the lumbar spinal cord were significantly lower ($p=0.012$) in the WBV group ($0.008\pm0.004$) than in the sham control group ($0.028\pm0.016$).
**Conclusions**: BiP has been shown to be modulated in association with other painful injuries. In fact, a painful facet joint injury upregulates BiP expression in neurons of the dorsal root ganglia. However, the current finding of decreased BiP in the spinal cord may suggest that cells in the spinal cord may be damaged by the WBV exposure, leading to the decrease in BiP. Additional studies are needed to define the time course of development of this change, as well as studies to define in which spinal cells these changes are occurring.

**A8.** Abstract accepted for presentation at SFN Mtg. in November, 2013.

## Painful whole body vibration induces increased expression of nerve growth factor & brain-derived neurotrophic factor in cervical intervertebral discs in a rat model

S. Kartha, M.E. Zeeman, H.A. Baig, B.B. Guarino, B.A. Winkelstein

Chronic neck pain is a common disorder with high costs, affecting many in the general population. Discogenic pain is a common source of pain and is hypothesized to originate when the typically aneural intervertebral disc (IVD) becomes innervated after injury or with degeneration. Spinal injury from whole body vibration (WBV) has been linked to low back and neck pain, with increased loading in the vertebral column and discs speculated as a potential pain source. Yet, the biochemical mechanisms leading to discogenic pain from its hyper-innervation and/or degeneration are unclear. Studies report upregulation of the neurotrophins, nerve growth factor (NGF) and brain-derived neurotrophic factor (BDNF), in lumbar degenerated IVDs. Because these growth factors mediate nerve growth they are believed to contribute to disc pain. Although there is increasing focus on defining the role of these factors in discogenic pain, work has largely focused on the lumbar discs, and no study has determined if similar mechanisms exist in the cervical spine. This study aimed to define if painful WBV induces changes in neurotrophins in the cervical IVDs. WBV was imposed along the spine's long-axis under inhalation anesthesia with the rat in the prone position. Vibration was applied for 30 minutes at 15Hz and 0.55g daily for 7 days followed by 7 days of rest. Sham rats underwent the same paradigm with anesthesia exposure only. Mechanical hyperalgesia was assessed prior to, during, and after the WBV exposure period. On day 14, cervical spines were harvested to evaluate NGF and BDNF mRNA and protein expression using RT-qPCR and western blot (n=8/group). Immunohistochemistry (n=4/group) was used to localize and quantify NGF and BDNF expression levels in different regions of the disc. WBV exposure induced behavioral hypersensitivity in the forepaw through day 14 that was not present in shams ($p<0.01$). In association with pain, WBV increased NGF and BDNF transcripts by 1.6-fold and 2.0-fold over sham, but not significantly. WBV did produce a significant ($p<0.006$) 5-fold increase in BDNF protein and a significant ($p<0.04$) 1.8-fold increase in the 75kDa NGF isoform. The 28kDa isoform of NGF increased 4.9-fold, but this was not significant. After WBV, both NGF and BDNF labeling significantly ($p<0.01$) increased in the inner annulus compared to the outer annulus of the disc. These findings suggest that painful WBV may induce similar patterns of upregulation of neurotrophins as in disc degeneration. Results also suggest that the same painful processes present in the lumbar spine may occur in the cervical spine and may explain one such potential mechanism responsible for the development of chronic neck pain.

This work was supported by a grant from the Department of Defense (W81XWB-10-2-0140).

**A9.** Abstract accepted for presentation at Philadelphia Spine Research Society Mtg in November, 2013.

# Upregulation of NGF & BDNF in cervical intervertebral discs exposed to painful whole body vibration

Sonia Kartha, Martha E. Zeeman, Hassam A. Baig, Benjamin B. Guarino, Beth A. Winkelstein*,#

Bioengineering & #Neurosurgery
University of Pennsylvania, Philadelphia, PA

* Contact: Beth A. Winkelstein, PhD, winkelst@seas.upenn.edu

**INTRODUCTION:** Whole body vibration (WBV) has been suggested as a cause of low back and neck pain due to the increased loading across the vertebral column and the intervertebral discs (IVDs). Discogenic pain is hypothesized to originate after injury or result from degeneration when the typically aneural IVD becomes innervated. Although the specific physiological mechanisms leading to hyper-innervation of the disc are unclear, upregulation of the neurotrophins, nerve growth factor (NGF) and brain-derived neurotrophic factor (BDNF), has been reported in degenerated lumbar IVDs. As such, because these growth factors mediate nerve growth there is growing support for the hypothesis that they contribute to the development of disc pain. However, while these growth factors have been characterized in the context of low back pain and lumbar discs, no study has determined if similar processes occur in the cervical spine in association with painful spinal loading.
**METHODS:** WBV was imposed in the rat directed along the spinal long-axis under inhalation anesthesia. Vibration was applied daily for 30 minutes at 15Hz and 0.55g for 7 days followed by 7 days of rest. Shams underwent the same procedures but only exposure to anesthesia. Mechanical hyperalgesia was assessed throughout the study. On day 14, cervical spines were harvested to evaluate NGF and BDNF mRNA and protein expression using RT-qPCR and western blot (n=8/group). Immunohistochemistry (n=4/group) localized and quantified NGF and BDNF immunoreactivity in different regions of the disc.
**RESULTS:** WBV exposure induced behavioral hypersensitivity in the forepaw through day 14 that was not present in shams ($p<0.01$). WBV significantly increased BDNF mRNA levels ($2.6\pm1.2$) over sham ($1.5\pm1.0$) levels ($p<0.04$). The transcript of mature NGF also increased 1.6-fold over sham, which was significant ($p<0.03$) WBV also significantly increased protein expression of both BDNF ($p<0.01$) and the 75kDa NGF ($p<0.05$) at day 14 by nearly 5 and 10-fold, respectively. Both BDNF and NGF exhibited greatest increases in the inner annulus and nucleus pulposus after WBV.
**CONCLUSIONS:** These findings indicate that painful WBV induces neurotrophin upregulation in the cervical IVD. Furthermore, the increased labeling in the inner annulus and nucleus pulposus is similar to those patterns observed in disc degeneration. It is possible that spinal loading during WBV prompts biochemical changes in the disc that may relate to pain.
**ACKNOWLEDGEMENTS:** This work was supported by a grant from the Department of Defense (W81XWB-10-2-0140).

**A10.** Sample images of muscle labeling.

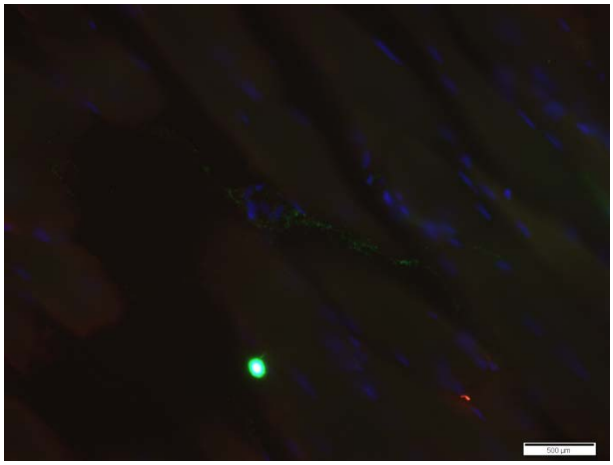

Green: CGRP, Red: BDNF; Blue: nuclei

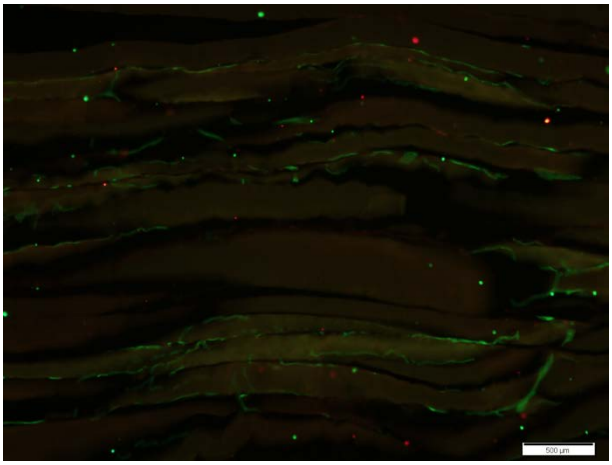

Green: IB4

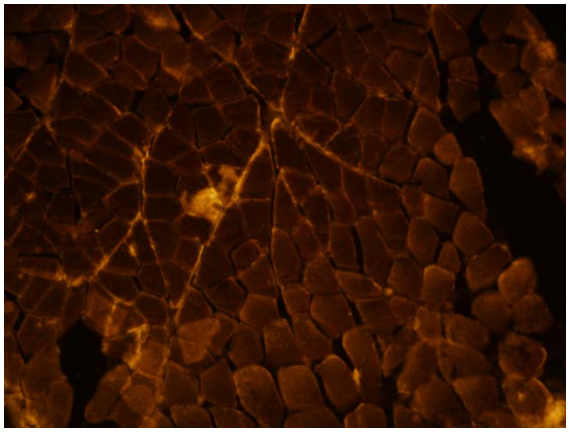

BDNF labeling

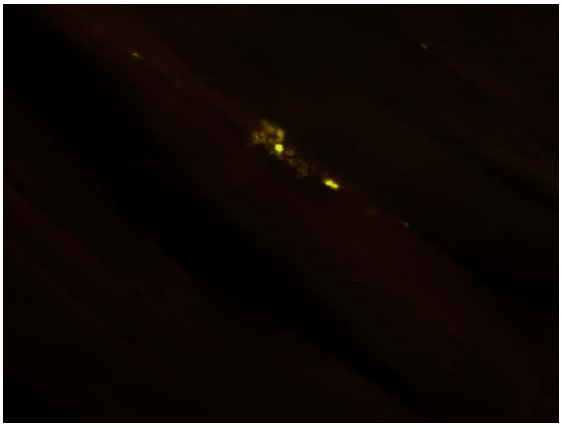

TNF

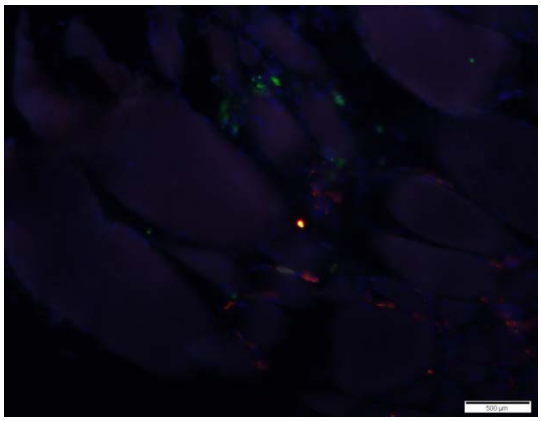

Green: ED1, Red: IBA1

**A11.** Serum cytokine levels compared to baseline for Days 1, 7, and 14.